UNIVERSIDADE DE LISBOA
FACULDADE DE CIÊNCIAS
DEPARTAMENTO DE QUÍMICA E BIOQUÍMICA

Evaluating the impact of 2D, 3D static and 3D microfluidic tissue culture conditions on the *in vitro* response of cancer cells to chemotherapeutic agents

Mariana Gaspar de Almeida

Mestrado em Bioquímica
Especialização em Bioquímica Médica

Dissertação orientada por:
Professora Doutora Margarida Gama-Carvalho, FCUL

2021

Acknowledgements

Firstly, I want to thank from the bottom of my heart to my supervisor Professor Margarida Gama-Carvalho. I will forever be grateful for the opportunity she gave me to work within a challenging project that I was so excited about. Her support every time the experiments did not go as expected. I would also want to thank for her excitement and complete commitment to this challenging project. Furthermore, I will thank to Professor John Greenman, who helped and made this project possible from the first day of my master. It was also of extreme importance the complete availability for each meeting and feedback every time we needed his expertise. It was only possible for me to pursue the microfluidic device testing because Professor John Greenman kindly sent to our lab his devices and components.

To my lab colleagues, I want to thank every advice, positive critics and ideas about my work and performance. I would like to specially thank Claúdia, for giving me the opportunity to discuss every single scientific detail with her, for making me part of her project and listening my naive thoughts about it, who showed me what being passionate about a career and life is, and for giving me a friend for life. Also, to Tânia, who was always available for every question and to chat with me and from whom I have learnt so much about balancing work and personal life.

To all people involved in this project and who directly participated and helped me to proceed with it I want to give my most participation and acknowledgment: Hugo Botelho for his amazing help with the microscopy analysis of my work, for the data analysis of the 2D immunofluorescence done by him and for his exceptional availability to help with every question; Luís Marques for his amazing availability to build a functional 3D spheroid immunofluorence protocol, for his many hours with me in the cryostat and microscopy and for always being available for solving every problem and question of mine; Gabriela Marques that provided us with her expertise; Sólveig Thorsteinsdóttir for kindly allowing me the usage of her lab for the immunofluorescence step; last but not least Luisa Romão and Cristina Carvalho who kindly provided us the HCT-116 and U87 MG cell lines, respectively.

To my friends that this university and master gave to me I would also like to thank them for the endless conversations about every step of this journey, the monthly dinners and for not feeling alone in this challenging period of my life.

To my best friends and boyfriend, Maria, Margarida, Manuel and Guilherme I want to thank them for being my chosen family and the ones that have been there for each tear, rage, laugh and smile that this journey gave me and for always making me remember that life is not just about work. I want to specially thank my boyfriend for each motivational talk and laugh that he gave me that made me remember who am and enjoy this beautiful journey.

To all my family who always gave me unconditional support and love. To my mum, who always asked me want she could do to help and who supported me and told me how proud she was of me every day. To my dad, who always questioned my ideas and perspectives to make me grow and improve, and who taught me to be better every single day in the best car rides of my life. To both of them for taughting me that even when the world falls around us, we are strong enough to fight for what we believe in. To my grandparents who made me feel loved and unique. To my brother for always making me feel a super sister and a role model, and for always making me rest at the end of the day by spending time with him.

Lastly, I want to thank each person involved in this process that made me grow and fight for what I believe in and made this project possible. Furthermore, I want to dedicate this thesis to my grandparents who I hope are very proud of their granddaughter.

Resumo

Apesar da evolução exponencial no campo da investigação médica e biomédica, o cancro continua a ser uma das principais causas de morte no mundo. É a sexta principal causa de morte no mundo com cerca de dez milhões de pessoas a morrerem por ano devido ao tratamento ineficiente desta doença. Um dos principais problemas da comunidade científica na descoberta de tratamentos mais eficazes e personalizados para cada paciente é a inexistência de modelos *in vitro* que sejam capazes de representar a complexidade de um tumor *in vivo*. Desta forma, é de extrema importância o contínuo esforço da comunidade científica na descoberta e desenvolvimento de modelos *in vitro* que representem cada vez melhor a complexidade dos processos biológicos presentes nos tumores humanos.

Em investigação científica, o método mais comum de cultura de células é o de duas dimensões (2D), que possibilita o estudo de mecanismos biológicos associados a doenças, bem como o teste de possíveis alvos e tratamentos. Este método baseia-se na utilização de frascos ou placas de *petri* de plástico como suporte para o crescimento de linhas celulares tumorais. As células são adicionadas ao frasco e é lhes adicionado o meio adequado com a respetiva suplementação de modo que estas consigam obter todos os nutrientes necessários à sua sobrevivência e duplicação. O meio é metabolizado pelas células e posteriormente removido e substituído por meio novo, para que as células possam continuar a crescer e a multiplicar-se. Assim, ao invés do que acontece no organismo humano com a presença do sistema circulatório, as células têm à sua disposição, de forma controlada, todos os nutrientes necessários à sua sobrevivência e a remoção dos produtos finais provenientes do metabolismo celular depende do operador. Assim, o método 2D representa uma forma bastante simples e com baixo custo de manter as células em cultura, motivo pelo qual é um dos mais utilizados em investigação científica. Desta forma, a cultura de células em 2D teve um impacto colossal na descoberta de muitos dos processos biológicos que conhecemos hoje em dia, essenciais para o desenvolvimento de terapias e tratamentos para variadas doenças. No entanto, a identificação e investigação de possíveis alvos quimioterapeuticos utilizando apenas este tipo de cultura celular apresenta uma taxa de reprovação de novos fármacos de cerca de 90%. Tal facto deve-se em parte à ausência de propriedades essenciais nos tumores *in vivo* como, organização tridimensional das células, as interações célula-célula, sinais bioquímicos e a presença de componentes essenciais do microambiente do tumor, que levam à exagerada simplificação dos mecanismos observados em tumores humanos. Desta forma, as células que crescem usando este método não irão responder de forma semelhante aos tumores presentes no organismo humano aquando da presença de agentes quimioterapeuticos, levando ao aumento da taxa de reprovação destes agentes.

A organização estrutural tridimensional presente nos tumores humanos é essencial para a organização, diferenciação e proliferação das células que compõem o tumor. Apesar da grande utilização de linhas celulares tumorais em conjunto com métodos 2D, células derivadas de tumores de pacientes (PDCs) e xenoenxertos de pacientes (PDXs) são exemplos de métodos usados numa tentativa de maior aproximação com a realidade dos tumores *in vivo.* No entanto, estes modelos ainda apresentam grandes falhas na representação das características estruturais dos tumores. Assim, foram desenvolvidos modelos tridimensionais (3D) que consistem na formação de esferóides ou organoides, agregados celulares, usando dois tipos de métodos de formação: com ou sem um esqueleto artificial ou natural a envolver as células. Este tipo de modelo representa melhor o ambiente tridimensional do tumor, uma vez que permite a interação celular causada pela agregação das células na formação da estrutura tridimensional e pode permitir a interação com um esqueleto que mimetiza a matriz extracelular (ECM) presente *in vivo*. A interação entre células cancerígenas e a ECM e outros componentes como fatores de crescimento e proteínas é essencial para a determinação da progressão tumoral e sobrevivência do tumor *in vivo*. Desta forma, é fundamental que a eficácia dos agentes quimioterapeuticos seja testada em modelos que sejam capazes de descrever estas interações e características de modo que o efeito detetado nos ensaios *in vitro* seja o mais parecido com o observado no paciente. Uma das principais vantagens

do uso de esferóides para o desenvolvimento de novas terapias é o facto deste tipo de estruturas apresentarem uma estrutura tridimensional em camadas, estando presentes células em proliferação na camada mais externa e células em senescência e necrose à medida que nos aproximamos do seu interior. Assim, a presença de células em diferentes estados do ciclo celular tem como consequência uma diferença na eficácia do tratamento em cada parte da estrutura tridimensional. Desta forma, os esferóides são capazes de mimetizar a heterogeneidade e mecanismos de resistência aos tratamentos *in vitro*. No entanto, apesar da grande evolução dos modelos *in vitro*, estas estruturas 3D ainda não representam na totalidade as características de um tumor no organismo humano. Assim, os dispositivos microfluídicos são uma das áreas de maior desenvolvimento de modelos *in vitro* para a testagem de novos tratamentos tumorais. Baseiam-se na adição aos modelos 3D de características como a perfusão de nutrientes e remoção de produtos do metabolismo celular e da pressão associada a este mecanismo. Este tipo de dispositivos permite a reprodução das funções do sistema circulatório do organismo humano *in vitro*, tendo a possibilidade de controlar a velocidade do fluxo de nutrientes e de remoção de produtos do metabolismo. Para além destas vantagens, possibilita também o estudo em tempo real dos esferóides com a análise do fluxo que sai destes dispositivos depois de passar pelas células, permitindo o desenvolvimento de terapias personalizadas em tempo real. No entanto, os sistemas microfluídicos ainda estão em desenvolvimento dada a sua complexidade e fácil perturbação com pequenos detalhes como a presença de bolhas de ar na câmara onde se localiza o esferóide.

Neste trabalho, pretendeu-se contribuir para a abordagem desta problemática com foco na utilização de duas linhas celulares, HCT-116 e U87 MG, de cancro colorectal e de glioblastoma, respetivamente. O cancro colorectal é o terceiro mais frequente no mundo, com quase 700 mil mortes por anos, e o glioblastoma é um dos tumores cerebrais mais agressivos do sistema nervoso central, necessitando ambos de terapias mais eficazes no seu tratamento. Assim, este estudo teve como objetivo comparar três métodos de cultura celular diferentes: 2D, esferóides e um sistema microfluídico, de forma a identificar diferenças na resposta celular a dois medicamentos quimioterapeuticos, 5-FU e TMZ utilizados no tratamento de cancro colorectal e glioblastoma, respetivamente. De forma a atingir este objetivo, as células cultivadas nos diferentes métodos foram avaliadas em termos de viabilidade celular, expressão génica, proliferação celular e organização tridimensional. Em termos de viabilidade celular, as duas linhas celulares apresentaram comportamentos diferentes, tendo a linha celular HCT-116 demonstrado que as células cultivadas em 2D apresentam uma viabilidade menor do que as 3D aquando do tratamento com 5-FU, enquanto a linha celular U87 MG não apresentou uma diferença significativa entre os dois métodos de cultura. Desta forma, parece que a elevada heterogeneidade característica de células de glioblastoma pode ter causado a ativação de mecanismos de seleção de clones resistentes ao tratamento, demonstrando assim um menor impacto do tratamento, independente do tipo de método de cultura utilizado. Relativamente à expressão génica, os resultados sugerem que o aumento da expressão de GADD45A e CDKN1A podem estar relacionamos com a resistência das células ao tratamento e, por isso, com uma maior viabilidade celular. A expressão génica do c-Myc sugere que o seu aumento pode estar relacionado com a baixa presença de oxigénio, permitindo a ativação de um mecanismo de resistência aos tratamentos, no entanto os resultados não foram consistentes, sendo necessário uma análise posterior mais detalhada. Em termos de organização espacial, os esferóides HCT-116 formados apresentavam uma camada externa proliferativa bem definida que foi afetada pelo tratamento, ao invés dos esferóides U87 MG, em que esta camada não se mostrou tão evidente e na qual o tratamento não mostrou ter impacto.

Em suma, este trabalho é uma contribuição para a identificação das principais diferenças, em termos de viabilidade celular, expressão génica e organização tridimensional, do método tradicional 2D e do método 3D utilizando esferóides na resposta a fármacos quimioterapeuticos. No entanto, apesar da necessidade de uma análise mais detalhada, os resultados parecem sugerir que a resposta celular a agentes quimioterapeuticos pode ser influenciada pelo método de cultura *in vitro* utilizado.

Palavras-chave: cultura celular 2D, cultura celular 3D, esferóides, viabilidade celular e expressão génica.

Abstract

Cancer is still a huge worldwide problem, and many cancer types still lack effective therapy. One of the major challenges in cancer and medical research is the transfer of knowledge from the wet lab to patient's treatment. This is partly due to the fact that *in vitro* cell culture models are still in need of development in order to better mimic the structural characteristics of human solid tumours and their interactions with the surrounding environment. This study aimed to compare the tumour cell's response to chemotherapeutic agents under three different culture conditions by assessing cell viability, gene expression, cellular proliferation, and structural arrangement. For this purpose, two cell lines were used, HCT-116 and U87 MG, one from colorectal cancer and the other from glioblastoma, respectively. The results showed that both cell lines have different behaviours. Indeed, while HCT-116 had higher cell viability in the 3D than in the 2D culture model upon 5-FU treatment, the U87 MG cell line had almost no difference between the two models, with a tendency of the 2D having higher viability. The results from GADD45A and CDKN1A gene expression followed a similar behaviour of the cellular viability, therefore a higher cellular viability may eventually be associated with a higher expression of these genes, and thus be related to possible resistance mechanisms. The spheroids formed by both cell lines presented good integrity and a typical 3D layered structure. Upon chemotherapeutic drug treatment, the HCT-116 spheroids showed a big impact in the size and distribution of the proliferative cells within the spheroid, however the U87 MG spheroids showed less evidence of TMZ treatment impact. In conclusion, this work gives important information about the molecular and structural differences between cells cultured in 2D and 3D cell culture conditions, which are therefore relevant for the development of drug screening methods.

Keywords: 2D cell culture model, 3D cell culture model, spheroids, cell viability, gene expression.

1. Índice

List of tables

List of figures

List of abbreviations

CRC	Colorectal cancer
TME	Tumour microenvironment
APCs	Professional antigen presenting cells
MSI	Microsatellite instable
CAF	Cancer-associated fibroblasts
TECs	Endothelial cells
ECM	Extracellular matrix
5-FU	5-Fluorouracil
FdUMP	Fluorodeoxyuridine monophosphate
FdUTP	Fluorodeoxyuridine triphosphate
FUTP	Fluorouridine triphosphate
TS	Thymidylate synthase
CIN	chromosomal instability
CIMP	CpG island methylation phenotype
GADD45A	Growth arrest and DNA-damage-inducible 45 alpha
FAS	Fas cell surface death receptor
BAX	BCL2 associated X
CDKN1A	Cyclin dependent kinase inhibitor 1A
GBM	Glioblastoma
CSCs	cancer stem cells
VEGF	vascular endothelial growth factor
TMZ	temozolomide
MTIC	5-(3-methyltriazen-1-yl)-imidazole-4-carboxamide
MGMT	O6-methylguanine-DNA methyltransferase
MMR	Mismatch repair
BER	Base excision repair
2D	Two-dimensional
3D	Three-dimensional
MF	Microfluidics
MTS	3-(4,5-dimethylthiazol-2-yl)-5-(3-carboxymethoxyphenyl)-2-(4-sulfophenyl)-2H-tetrazolium, inner salt
cDNA	Complementary DNA

2. Introduction

2.1. Cancer biology

Cancer is the second leading cause of death globally and one of the most serious diseases around de world (Neufeld et al., 2021; B. Zhang et al., 2007). The National Cancer Institute (NCI-USA) defines cancer as the name given to a collection of related diseases that have in common the fact that some of the body's cells begin to divide without any control and spread into surrounding tissues.

Usually, when human cells get old or damaged, they die and are replaced by new cells grown from healthy cells that suffered division, being this process regulated by the human body needs. However, in the presence of cancer, this orderly process breaks down and abnormal cells survive, stopping the production of new and healthy cells. The uncontrolled growth of these damaged cells, influenced by multiple factors that can either promote cancer progression or inhibit it, may lead to the formation of solid cell aggregates, the tumours (*What Is Cancer? - National Cancer Institute*, n.d.; B. Zhang et al., 2007). Although there are many different types of cancers, all cancer cells have some unique features: self-sufficiency in growth signals, insensitivity to growth-inhibitory signals, evasion of programmed cell death (apoptosis) and limitless replicative potential (Hanahan & Weinberg, 2000; Maira et al., 2007). Furthermore, it is common that cancer cells are able to avoid or survive the immune killing processes by slowing down immune reactions or stopping them and by the selection of less immunogenic cancer cells, allowing them to live and pass this feature to the next generation (Messerschmidt et al., 2016; *What Is Cancer? - National Cancer Institute*, n.d.). In addition, cancer cells can also influence surrounding normal cells, blood vessels and molecules, in order to get what they need to grow and to spread, forming metastases. This process involves sequential orchestration of complex biological mechanisms, which begins with the digestion of the extracellular matrix, caused by an up-regulation of specific molecules, followed by the migration and integration into the blood vessels, and finally the arrival and take up of the cancer cells into distant organs. Moreover, this cancer mechanism is responsible the development of distant metastases that cause 90% of the cancer deaths (Harrington, 2016).

In this work we focused on two main cancer types: the colorectal cancer (CRC) and the glioblastoma, the first one being the third leading cause of cancer death in the developed world and the latest the most malignant adult brain tumour (Kahlert et al., 2017).

2.1.1. Tumour microenvironment

The tumour's environment has an important role, since tumour cells have the ability to send and receive signals that will have an impact on the local tissues and neighbouring cells and will determine their progression (Devarasetty et al., 2020). The tumour's structure is characterized by a disorganized tissue formation that occurs within organs, with the presence of stroma that influences the evolution of cancer cells. However, the main research and therapeutic strategies for prognostication of the patient are linked to the analysis of isolated tumour cells in order to assess proliferation and morphology. Although these measurements are correlated to tumour progression, they do not have into account the interactions between the tumour and its surrounding environment. Therefore the development of new technologies that take into account the importance of the tumour microenvironment (TME) will have a huge impact on patient mortality (Devarasetty et al., 2020).

The TME of a specific tumour is a highly complex environment that is composed by a variety of cells (**Figure 2.1**). Besides the presence of tumour cells, immune cells are also present in tumours, including macrophages, natural killer cells and lymphocytes, and other cells too, such as endothelial cells and stroma cells. All these types of cells interact with each other and determine the tumour's natural

progression. Mainly, the immune cells show an important role in establishing the metastatic and invasive ability of the tumour, since depending on their interaction with other components and their tumour's infiltration they can lead to different outcomes in the tumour progression. Therefore, the composition and organization of the TME is directly associated with the clinical outcome of therapies applied to cancer patients (Giraldo et al., 2019). The role of immune cells present in the TME is directly related to the molecules that they express, like cytokines or ligands. The most common anti-tumour immune cell is the CD8+ T lymphocyte that recognises tumour cells in an antigen-specific manner, therefore secreting cytotoxic molecules to kill them (Giraldo et al., 2019). However, for this detection to happen the CD8+ T cells have to be "taught" by professional antigen presenting cells (APCs), a mechanism that usually takes place in secondary lymphoid organs, although it is now known that this process also occurs within the tumoral tissue. One of the main examples of the immune response induced by tumour cell mutations is microsatellite instablility (MSI) in colorectal cancer (Giraldo et al., 2019). This subtype of cancer has an increased infiltration of CD8+ T cells due to its increased rate of mutagenesis. Besides the immune components, the TME has also, as mentioned, important non-immune components. The vascular network of the tumour, promoted by the hypoxic environment and, therefore, the production of proangiogenic factors, is fundamental for the development of the tumour (Giraldo et al., 2019). Other main non-immune cell components are the cancer-associated fibroblasts (CAF), which have been reported to regulate multiple aspects of the tumorigenesis, such as growth, survival, and immune cell recruitment. Furthermore, these cells also enhance angiogenesis by the secretion of factors that activate endothelial cells (TECs) (Chen et al., 2020). Abnormal TECs can lead to a disordered vascular TME, affecting the tumour's metabolism and drug resistance mechanisms. In addition, CAF often form part of an complex and thick arrangement of cells and stromal matrix surrounding the tumour, which represents a physical barrier for cytotoxic immune cell infiltration (Giraldo et al., 2019). Moreover, it has been shown that the combination of paracrine factors, stromal cells, tumour associated fibroblasts and extracellular matrix (ECM) gives rise to a perfect environment for the cancer to thrive and escape the treatment. Furthermore, it was found that the organization of the collagen ultrastructure into the tumour influence radically the behaviour of the tumour cells, being that a structured ECM seems to induce chemoresistance in cancer cells (Devarasetty et al., 2020).

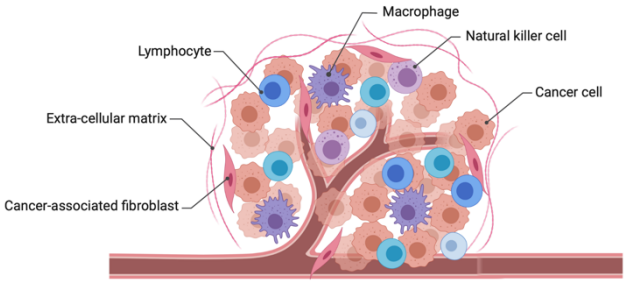

Figure 2.1 – Representation of the tumour microenvironment with the presence of immune and non-immune cells, and the vascular structures associated to it. The presence of different type of cells in the surroundings of the tumour is of extreme importance for the progression of the tumour. Created in Biorender.com.

Therefore, the study and understanding of the TME components and the development of *in vitro* models that take into consideration the presence and importance of these molecules and that replicate the context of whole-body physiology are of extreme importance (Chen et al., 2020; Devarasetty et al., 2020). In addition, the challenge facing tumour immunology is how to translate these new highly complex findings into relevant, simple and consistent biomarkers to use in clinical settings (Giraldo et al., 2019). Although, in this present study, the cell culture methods do not use an extracellular matrix nor the presence of different cell types in culture, it is extremely important the development of knowledge in this field in order to find a better *in vitro* tumour model, hence the reason for this section. Furthermore, comprehensive analysis of the multiple exchanges between tumour cells and their surrounding microenvironment is essential for the development of new targeted therapies and to predict the side-effects of the treatment and tumour progression (Baghban et al., 2020; Chen et al., 2020; Devarasetty et al., 2020).

2.2. Colorectal Cancer

Colon is one of the fundamental parts of the digestive tract, with the main functions being the absorption of water, minerals, and nutrients and to serve as storage area for the waste material that forms the faeces (Arvelo, 2015). Furthermore, because of its biological function, it has a high level of cellular regeneration, which increases the probability of developing diverse pathologies (Arvelo, 2015).

Colorectal cancer is the third most frequently diagnosed cancer in the world, with between one and two million new cases being diagnosed every year and 700.000 deaths per year (Mármol et al., 2017; Passardi et al., 2020). 90% of the diagnosed cases are in adult patients, being considered as the second cancer diagnosed in women and the third in man (Sagaert et al., 2018). There is a geographic correlation of the cases' prevalence, with developed countries being the most affected ones. This relation can be explained by the key role that environmental factors play in the development of colorectal cancer, such as meat and alcohol consumption and smoking habits. In contrast, habits associated to a healthy life, such as vegetable consumption and physical activity, are linked to a decrease of CRC incidence (Sagaert et al., 2018). However this tendency is changing since countries from other parts of the globe have acquired habits more similar to developed countries in the past years (Mármol et al., 2017). Furthermore, hereditary factors, revealed by family history, history of polyps in the colon or personal history of cancer, are also involved in the occurrence of the type of cancer (Sagaert et al., 2018). Moreover, older ages are a main personal characteristic that represent a risk factor of suffering from CRC, being the probability extremely increased past the age of fifty (Mármol et al., 2017).

In general, CRC is diagnosed at advanced tumour stages due to the rapid formation of metastasis and the high rate of transfer through the bloodstream, which cause a main problem in achieving a more effective treatment (Arvelo, 2015). CRC can be divided into three main types accordingly to their origin and expression. The sporadic form, in which an individual develop a point mutation that causes the disease during life, without caring any mutation which makes them susceptible to develop this cancer and have any type of family link, is the most common one, accounting for 70% of all colorectal cancers (Arvelo, 2015; Mármol et al., 2017). The familial type is when there is no mutation associated but members of the patient's family have suffered from CRC and, in this case, environmental factors play a critical role in determining the development of the cancer (Arvelo, 2015). The last type of cancer is the hereditary type that can be characterized by the presence of inherited mutations that affects one of the gene alleles. Therefore, a development of a point mutation during life in the other gene allele will led to cancer development (Arvelo, 2015). The therapeutic strategy used in each patient is highly dependent on the stage of the cancer, which is determine by the TNM system, developed by the American Joint Committee on Cancer and the Union for International Cancer Control, where the tumour invasion (T), the affected lymph nodes (N) and the presence of metastasis (M) are assessed (Sagaert et al., 2018). Moreover, in spite of the advances in CRC therapeutics, the survival rates remain extremely variable depending on the patient's tumour (Sagaert et al., 2018). Some of these differences can be explained by the heterogeneity of this type of cancer tumours. Furthermore, recent research into the different molecular processes involved in CRC development are shifting the therapeutics to the use of personalized medicine (Sagaert et al., 2018).

The most important chemotherapeutic molecule currently used in CRC treatment is 5-fluorouracil (5-FU), which is used worldwide in the treatment of metastatic colorectal cancer, either alone or in combination with other drugs (Blondy et al., 2020; P. M. De Angelis et al., 2006). 5-FU is an analogue of uracil with a fluorine atom at the C-5 position in place of an hydrogen (Longley et al., 2003). After being administered intravenously to the patient, the drug is converted intracellularly into several active metabolites: fluorodeoxyuridine monophosphate (FdUMP), fluorodeoxyuridine triphosphate (FdUTP)

and fluorouridine triphosphate (FUTP) (Blondy et al., 2020; Longley et al., 2003). After this conversion, these metabolites will disrupt RNA synthesis and inhibit the action of thymidylate synthase (TS) (Longley et al., 2003) (**Figure 2.2**). TS is an enzyme that catalyses the dUMP to dTMP conversion, providing a *de novo* source of thymiadylate, necessary for DNA replication and repair (Longley et al., 2003). In the presence of 5-FU, the active metabolite FdUMP binds to TS forming a stable complex, thereby inhibiting its normal function and synthesis of dTMP (Longley et al., 2003). The elimination of dTMP, and subsequent depletion of dTTP, will cause perturbations in the levels of the other deoxynucleotides, meaning a severe disruption of DNA synthesis and repair (Longley et al., 2003). In addition, TS inhibition results in the accumulation of dUMP, which may lead to increased levels of dUTP (Longley et al., 2003). Both dUTP and FdUTP can be mis-incorporated into DNA and the repair of this event, in the presence of high (F)dUTP/dTTP ratios, by the UDG enzyme is pointless (Longley et al., 2003). Therefore, the resulting high number of DNA repair mechanism cycles, in order to try to maintain the genomic stability, will lead to DNA strand breaks and cell death (P. M. De Angelis et al., 2006; Longley et al., 2003). Some of the resistance mechanisms to 5-FU are associated with the overexpression of dTTP and with alterations of genes related to cell cycle and apoptotic pathways (P. M. De Angelis et al., 2006).

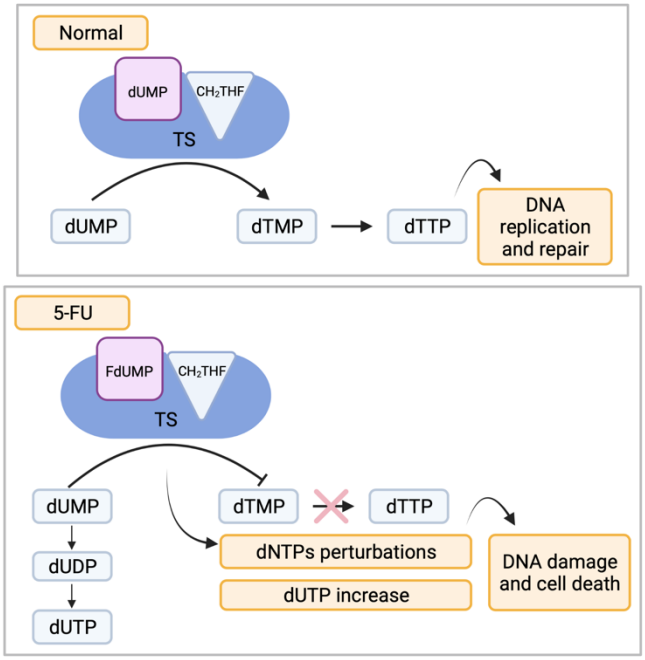

Figure 2.2 - Representation of the mechanism of action of the 5-FU in the thymidylate synthase (TS) in cells after its conversion into its active metabolites. The presence of 5-FU leads to the inhibition of TS and, consequently to the accumulation of dUMP and decrease of dTTP. This will affect the concentration of other dNTPs and an increase of dUTP. The misincorporation of dUTP in the DNA will later activate multiple DNA repair mechanisms and lead to cell death. Adapted from (Longley et al., 2003) and created in BioRender.com.

Mutations in oncogenes, tumour suppressors genes and DNA repair genes can lead to the development of CRC, as it also happens in other types of cancer (Mármol et al., 2017). Furthermore, genomic instability is a very important feature of colorectal cancer, having mainly three pathways, chromosomal instability (CIN), microsatellite instability and CpG island methylation phenotype (CIMP) (Mármol et al., 2017). The tumour suppressor protein p53 is the central hub of a complex molecular network, coordinating major cellular responses to potentially oncogenic stimuli, being that approximately 80% of advanced CRCs present TP53 mutations, mostly ones that decrease its DNA-binding ability, contributing to tumour aggressiveness and invasiveness (Ramos et al., 2021). TP53 function relies mainly in the sequence-specific transcriptional regulation of multiple target genes, mostly associated with cell cycle, apoptosis, DNA repair and senescence (Ramos et al., 2021). Among other things, chemotherapies promote apoptosis through induction of the tumour suppressor gene p53 (Longley et al., 2003). The disruption of the p53 pathway, mostly by TP53 mutation or p53 inhibition through interaction with negative regulators, is a major pathological event in local and advanced CRC (Ramos et al., 2021). This gene maintains DNA integrity by transcriptionally activating genes such as CDKN1A and GADD45A, which will induce cell-cycle arrest in response to DNA damage (Longley et al., 2003). However, depending on the type of DNA damage, this gene can also induce the action of apoptotic genes, such as FAS and BAX (Longley et al., 2003). *In vitro* studies have reported that loss of p53 function reduces cellular sensitivity to 5-FU, but some clinical studies have found that p53

overexpression is correlated with resistance to this drug. Studies using two 5-FU-resistant cell lines with the same TP53 genotype characteristic of the parental cell line, show that negative growth-regulatory genes, such as CDKN1A and GADD45A, and also genes related to apoptosis and DNA repair, are up-regulated when compared to the parental HCT-116 cell line (P. De Angelis et al., 2004). However, other studies show a small difference in the expression of negative growth-regulatory genes between the 5-FU-resistant cell lines and the parental one (P. M. De Angelis et al., 2006). For this reason, it is still difficult to understand the role of these genes in the resistance mechanism to 5-FU. However, since the majority of the studies show a modification in p53 expression or p53 target-gene expression, it is possible to conclude that the arrest mechanism of 5-FU in CRC cells it is probably mediated by p53 (P. M. De Angelis et al., 2006).

Finally, it is still necessary to develop research on this type of cancer, in order to uncover the mechanisms that CRC relies on for tumour progression and resistance processes. This will support the discovery of new and more targeted therapies that will help optimizing the treatments and decrease the number of deaths (Arvelo, 2015).

2.3. Glioblastoma

Glioblastoma (GBM) is the most common and aggressive malignant form of the glial tumours of the CNS, being associated with extremely poor survival (Kesari, 2011; Stoyanov et al., 2018). The main characteristics of this type of cancer are uncontrolled proliferation, diffuse infiltration, necrosis, high angiogenesis, resistance to apoptosis, genomic aberrations and endothelial proliferation, resulting in a grade IV brain tumour by WHO (Kesari, 2011; Wirsching et al., 2016). The prognosis of patients with GBM is one of the dimmest, as the survival rate is one of the worst of cancer (Stoyanov et al., 2018). GBM accounts for 45,6% of primary malignant brain tumours and the survival is directly linked to age, having only a 5 year survival rate of 3% in patients aged 65 or older (Wirsching et al., 2016). Most of the patients with glioblastoma die in less than 1 year after diagnosis, in part as a result of chemoresistance associated with a cancer stem cell population, and the diffuse nature of the tumour (Musah-Eroje & Watson, 2019). The main risk factor associated with this type of cancer is age, with currently no established role for specific extrinsic factors (Wirsching et al., 2016).

Glioblastoma has an extremely wide set of alterations, both genetic and epigenetic, with many mutations having an established role in independent patient survival and treatment response (Stoyanov et al., 2018). There are two main types of glioblastoma, the primary one, which occurs *de novo*, without any evidence of a pre-existing malignant precursor, which affects the majority of patients, and the secondary one that occurs through progression of a low-grade astrocytoma (Kesari, 2011). The most common treatments for GMB are surgery, radiotherapy, and chemotherapy, although the cure was still not reached to most patients, due to the fact that GBM tumours have a distinct heterogeneity and present a high likelihood of a rapid and aggressive relapse (Kesari, 2011). Therefore, it is important to understand the molecular genetics of brain tumours in order to uncover predictive biomarkers and pathways involved in tumour progression and, thus developing more target and efficient therapies (Kesari, 2011).

One of the main challenges in GBM is overcoming the resistant cancer stem cells (CSCs) and multiple interactions with the TME. CSCs have the ability to self-renew and to differentiate into a variety of nontumorigenic cells within the tumour (Kesari, 2011). They are believed to play a crucial role in malignant glioma tumour initiation, progression and angiogenesis and are also relatively resistant to standard treatments (Kesari, 2011). Therefore, one of the main interests in glioma research is the identification of drugs that can target these CSCs. In addition, vascular endothelial growth factor (VEGF) was also found to be expressed by the CSCs, promoting angiogenesis and the need for vascular machinery (Kesari, 2011). In terms of the TME relation within the tumour, gliomas express tumour-

associated and tumour-specific antigens that should be recognized by the immune system, however they show a profound immunosuppression (Kesari, 2011). This may be due to cell-to-cell mechanisms and secretion of products that will result in T-cell activity inhibition, but these mechanisms are not yet fully understood. The cells within the glioblastoma can differ from individual gliomas in their morphology, genetics and biological behaviour. This heterogeneity of GBM is one of the challenges faced in treating the disease, since some tumour cells within the tumour itself may respond differently to a particularly therapy (Kesari, 2011). Furthermore, this heterogeneity can be due to clonal evolution, in which the more adaptive clones survive under selective pressures, such as drug treatment, and produce different mutations, or due to CSCs indefinitely division and differentiation into various types of cells (Kesari, 2011). Furthermore, experimental data suggests that adult glioblastoma may be derived from the small pool of adult neural stem and progenitor cells located in perivascular and hypoxic niches of the brain (Wirsching et al., 2016).

Temozolomide (TMZ), a DNA-alkylating agent that causes persistent DNA strand breaks and replication fork collapse, is currently used as the first-line chemotherapeutic drug for GBMs (Ye et al., 2021). TMZ is an oral alkylating agent that is absorbed intact, then undergoing spontaneous breakdown, forming MTIC (5-(3-methyltriazen-1-yl)-imidazole-4-carboxamide). Then, the MTIC will interact with water giving rise to highly reactive methyldiazonium ions (J. Zhang et al., 2012). The negatively charged DNA will act as a nucleophile and the methyl group from the ions formed is transferred to DNA bases, preferentially at the N7 position of guanine and at N3 adenine and O6 guanine residues, only affecting single stranded DNA (Stoyanov et al., 2018; H.-H. Wang et al., 2017; J. Zhang et al., 2012). The cytotoxicity of this compound is mainly due to the formation of O6-MeG, which will result in the insertion of thymine instead of cytosine during DNA replication. These unrepairable mutations induce the formation of single and double stranded DNA breaks resulting in cell cycle arrest and apoptosis (Singh et al., 2020).

The MGMT (O6-methylguanine-DNA methyltransferase) promoter methylation is used as predictor of the benefit of temozolomide chemotherapy in newly diagnosed and recurrent glioblastoma (Wirsching et al., 2016). It is considered the most important contributor to TMZ resistance, due to its direct role in counteracting DNA alkylation damage (Singh et al., 2020). MGMT is an endogenous DNA repair enzyme that helps maintain genomic stability through mismatch repair (Singh et al., 2020). Under TMZ treatment, MGMT can remove the methyl group in O6-methylguanine, neutralizing the drug-induced DNA damage (Singh et al., 2020). Therefore, MGMT expression, which is influenced by the methylation status of the MGMT gene promotor, is important in TMZ treatment response (Kesari, 2011; Singh et al., 2020). The hypermethylation of the promoter region causes a decrease in MGMT and it has been found that 40% of glioblastoma cases have the MGMT promoter methylated (Kesari, 2011; Singh et al., 2020; Wirsching et al., 2016). The mismatch repair system (MMR) is a DNA repair mechanism that works by correcting any mismatched nucleotide base pairings during DNA synthesis (Singh et al., 2020). Since the TMZ functions during DNA replication, under normal conditions the MMR machinery is recruited, generating breaks in the newly synthesized DNA strand (Singh et al., 2020). Repeated cycle of these breaks, just recognized in the daughter strand, resulting in futile cycles of thymine re-insertion, cause replication blockage and irreparable damage in DNA strands, leading to apoptosis (Singh et al., 2020; J. Zhang et al., 2012).The BER (base excision repair) pathway is responsible for repairing single nucleotide modifications, involving several enzymatic reactions (Singh et al., 2020). Most of the N7-guanine and N3-adenine methylations caused by TMZ treatment are recognized by the BER machinery, therefore mutations in components that either regulate or participate in this pathway increase the potential of TMZ cytotoxicity (Singh et al., 2020).

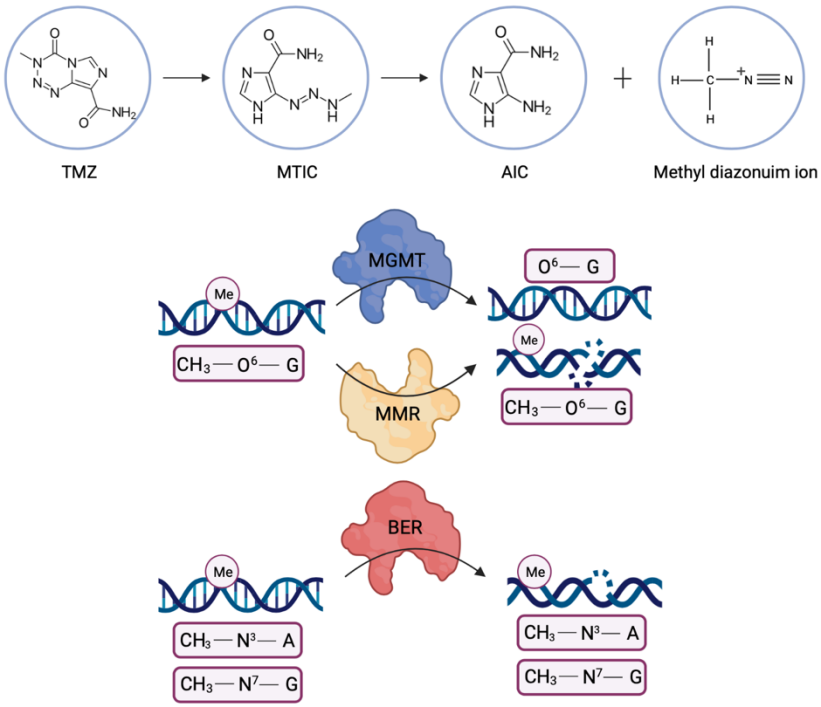

Figure 2.3 – TMZ metabolism within the cell and the influence of its active metabolites in the cell DNA and cell cycle. The TMZ will be transformed into diazonium ions that will have the ability to give a methyl group to the negatively charged DNA. This methylation can be repaired by three: MGMT, MMR and BER by different molecular processes. Therefore, mutations and activity of the components of these processes are linked with TMZ treatment resistance. MGMT - O6-methylguanine-DNA methyltransferase, MMR - mismatch repair, BER - base excision repair. Adapted from Singh et. Al, 2020 and created in BioRender.com.

In spite of the efficiency of TMZ in crossing the blood brain barrier and the increase in survival associated to the use of this drug, the prognosis of GBM remains unsatisfactory, since some patients show resistance to TMZ therapy (H.-H. Wang et al., 2017). TMZ has been reported to cause cell cycle arrest in the G2/M phase and to mediate apoptosis (H.-H. Wang et al., 2017). However, over 40% of the patients that receive this therapy have tumour progression, mainly due to intrinsic or acquired resistance to TMZ (Ye et al., 2021).

The transcription factor GATA4, which is a negative regulator of astrocyte proliferation, is lost in the majority of the GBM specimens and it was found that its re-expression in GBM cells sensitizes them to temozolomide, irrespective of MGMT status (Kesari, 2011). Wang et al., 2007 showed that, in response of TMZ treatment, some cell cycle and apoptosis genes were upregulated, such as GADD45A (H.-H. Wang et al., 2017). The knockdown of this gene was shown to be followed by an increase of p21 and increased cell death caused by the TMZ treatment in TMZ- resistant and TMZ-sensitive cell lines (H.-H. Wang et al., 2017). Moreover, the knockdown of GADD45A also caused a substantially decrease of MGMT expression in the same cell lines (H.-H. Wang et al., 2017). Furthermore, it was conclude that GADD45A plays a protective role against TMZ treatment through TP53-dependent and MGMT-dependent pathways in both resistant and sensitive TMZ cell lines (H.-H. Wang et al., 2017). The p21 protein, encoded by the CDKN1A gene, has a critical role in halting cellular proliferation, acting usually as a tumour suppressor, and is implicated in the response to many cancer treatments. However, recent studies showed that, under certain conditions, p21 could promote cellular proliferation and oncogenicity, revealing that it can have antagonistic cellular roles (Ye et al., 2021). Furthermore, p21 is considered an important molecular mediator of senescence, having an important role in inducing therapy-induced senescence. Therefore, TMZ-induced senescence is also dependent on p21 induction (Ye et al., 2021).

In summary, the incorporation of the new research developments and resulting target therapies into the clinical field is of extreme importance, in order to enable more individualized and in particular, more effective therapies for GBM (Kesari, 2011).

2.4. Anticancer drug screening - *In vitro* cancer models

It is estimated that around 30 to 40% of cancer patients are being treated with ineffective drug treatments (Neufeld et al., 2021). One of the major challenges for the development of novel treatments is the translation of scientific knowledge from the laboratory to the patient (Drost & Clevers, 2018). In spite of the increase in the number of potential anti-cancer agents being advanced for development over the past years, the number of these products that actually progress successfully throughout clinical trials is approximately 10% (Breslin & O'Driscoll, 2013). Ideally, the compounds that are potentially ineffective or have an unacceptable toxicity profile, which are the main causes of drug failures during development, should be dismissed as early as possible (Breslin & O'Driscoll, 2013). However, this remains a problem in large part due to the fact that the commonly used *in vitro* models poorly recapitulates the tumour characteristics (Drost & Clevers, 2018). Furthermore, in order to produce reliable biomedically relevant information it is necessary that the cells used *in vitro* mimic the phenotype of cells within the target tissue (Breslin & O'Driscoll, 2013). Commonly used human cancer models include cancer cell lines and patient-derived tumour xenografts (PDXs). The cancer cell lines show several drawbacks, such as the fact that they are performed in monolayer, and they need extensive and inefficient adaptation to the *in vitro* two-dimensional (2D) culture conditions, respectively (Drost & Clevers, 2018; Luca et al., 2013) The PDXs are able to retain the tumour heterogeneity and resemble the tumour cellular complexity, but they show some downsides such as, low implantation-take rates in hosts and higher cost (Gunti et al., 2021). Therefore, it is necessary to improve *in vitro* cell-based testing methods for a more informed prediction of drugs candidate efficacy and safety, and thereby reject poorly functioning compounds while prioritising promising candidates (Breslin & O'Driscoll, 2013). Moreover, the development of new and targeted therapies is essential to decrease the number of cancer deaths by preventive and personalised measurements (Drost & Clevers, 2018).

2.4.1. 2D culture method

The 2D (two-dimensional) culture method has been the method used since the early 1900s and it has played a vital role in biological research (Jensen & Teng, 2020; Souza & C Ferreira, 2016). After its development by Harrison, substantial improvements have been made on this type of culture (Jensen & Teng, 2020; Souza & C Ferreira, 2016).

In the traditional 2D cell culture method, cells grow as a monolayer on a flat surface, such as culture flasks or petri-dishes, the media is added as a source of nutrition and it is usually supplemented with bovine serum to help the cell growth (Breslin & O'Driscoll, 2013). When reaching confluence, the cells are sub-cultured in order to give them more nutrients and avoid senescence (Breslin & O'Driscoll, 2013). The culture containers used enable the cells to be fed easily and have space for them to grow, synthetic culture media, which have a direct impact in the development, nutrition and differentiation of the cells, can be supplemented to properly nourish the cells, and antibiotics or anti-fungal agents suitable for cell cultures can be used to prevent contaminations (Breslin & O'Driscoll, 2013; Souza & C Ferreira, 2016). Therefore, the 2D culture method still remains as the most commonly used *in vitro* method for therapeutics screening due to its simplicity, reproducibility and low cost (Nunes et al., 2019). The huge contribution of immortalized tumour cell lines grown under 2D culture models to the current knowledge about the molecular mechanisms of cancer and other diseases is also undisputed (Antoni et al., 2015). However, this added value is not so visible when it comes to drug approval, since drugs tested using the

2D cell model have a 95% failure rate, proving it to be a poor drug development model (Antoni et al., 2015). These statistics are due to the fact that flat 2D cell culture is unable to reproduce the properties of *in vivo* solid tumours since the tissue specific architecture, cell-cell interactions, mechanical and biochemical signals are lost under the simplified conditions (Jensen & Teng, 2020; Nunes et al., 2019; Souza & C Ferreira, 2016). Furthermore, the monolayer morphology only allows a portion of the cell membrane to contact with neighbouring cells, the cells are not allowed to pile on top of each other and the microenvironment is not physiologically relevant, since oxygen, nutrient or waste gradients and extracellular matrix are absent (Antoni et al., 2015). In addition, the cells in the body are continuously perfused by the blood stream, which makes a clear difference between the environment of the cells in a monolayer culture bathed by culture medium and a three-dimensional complex structure nurtured by the blood stream (Li & Cui, 2014; Souza & C Ferreira, 2016).

In consequence, a large number of ineffective drugs are able to proceed to *in vivo* assays, contributing to overuse of animals, as well as to increasing the time and overall cost of the drug discovery process (Nunes et al., 2019). In this way, aiming to mimic the cellular characteristics of an *in vivo* environment and to reproduce more closely the three-dimensional (3D) features of human tumours, new methodologies and *in vitro* models have been investigated and developed (Nunes et al., 2019; Souza & C Ferreira, 2016).

2.4.2. 3D culture method

Traditional 2D cultures have some drawbacks since they lack the diversity of internal spatial organization, presence of different cell types and presence of TME. Conversely, although animal models can better simulate physiological conditions, they are associated with a high cost and low rate of success in clinical trials (Chen et al., 2020).

Living organisms are three-dimensional arrangements of cells with complex cell-cell and cell-matrix interactions and complex transport dynamics of nutrients and cells. *In vivo*, the cells are maintained in a chemeostatic environment with a constant flow of new nutrients and removal of the waste products due to the presence of the circulatory system. Therefore, it is of extreme importance that the cell culture models used in research take into account the spatial organization of cells in tissues and their interactions (Antoni et al., 2015). The 3D cell culture system represents an important advance in cellular biology studies, since relevant biological aspects of the *in vivo* structures can now be better represented in *in vitro* models (Souza & C Ferreira, 2016). Although this technique has received more attention in the scientific community in the last years, the first references to it date back to the beginning of the 20th century. Indeed, the direct relation between cell proliferation and growth medium availability was first reported by Carrel in 1912, when he noticed that the central region of his cell colonies presented a high incidence of necrosis, and to solve this, he used silk treads as a scaffold for cell growth and development, describing what could be the first three-dimensional cell culture method (Souza & C Ferreira, 2016).

One of the most important characteristics of human solid tumours is their 3D architecture, since it provides optimal conditions for cellular organization, proliferation, and differentiation (Nunes et al., 2019). Therefore, three-dimensional cell cultures mimic to a certain degree the *in vivo* situation by allowing cell aggregation to form tissue spheroids, either naturally or by embedding cells on defined scaffolds that mimic the extracellular matrix of structural proteins (Li & Cui, 2014). This culture model allows the physiological cell-cell and cell-matrix interactions to regulate proliferation and differentiation in both space and time, maintenance of tissue function and homoeostasis (Li & Cui, 2014).

Three-dimensional culture models can be established using different approaches depending on the type of experiment being performed (Jensen & Teng, 2020). The two main 3D methods developed are spheroids and organoids, being the first one described above in section 2.4.2.1 since is the used model

of this project. The organoids are cells grown in 3D that are able to form structures similar to an organ in structure and function. These types of structures are formed by stem cells, pluripotent cells, tumour cells or tissues that will be subject to differentiation of the cells upon physical and chemical stimuli in the presence of a scaffold (Gunti et al., 2021). Nowadays, two major types of methods are available, one being scaffold-based and the other scaffold-free. In scaffold-based 3D cultures, cells grow anchored to 3D platforms that will mimic the ECM structure which can be classified as natural, semi-synthetic or synthetic biomaterials. In contrast, the ECM present in the scaffold-free based 3D cell culture is composed of proteins produced by cells during the formation of the culture. In the latter, the cultures are formed by cellular aggregates commonly known as spheroids (Costa et al., 2016).

Scaffold-based techniques (**Figure 2.4**) such as hydrogel-based support, polymeric hard material-based support, hydrophilic glass fibber and organoids have several advantages (Jensen & Teng, 2020). These methods are based on promoting the cells to grow on artificial 3D structures, where cells attach, migrate, and fill the interstices within the structure (Nunes et al., 2019). Firstly, hydrogels have unique features, since they show ability to mimic the EMC while allowing soluble factors, such as cytokines and growth factors to travel through the tissue-like gel (Jensen & Teng, 2020). Furthermore, these structures are also used to form spheroids that can be prepared in multiple ways depending on the experiment. Both natural and synthetic hydrogels exist, having different applications, but both represent a powerful tool to study cell-to-ECM interactions due to the ability to replicate the ECM structure (Jensen & Teng, 2020).

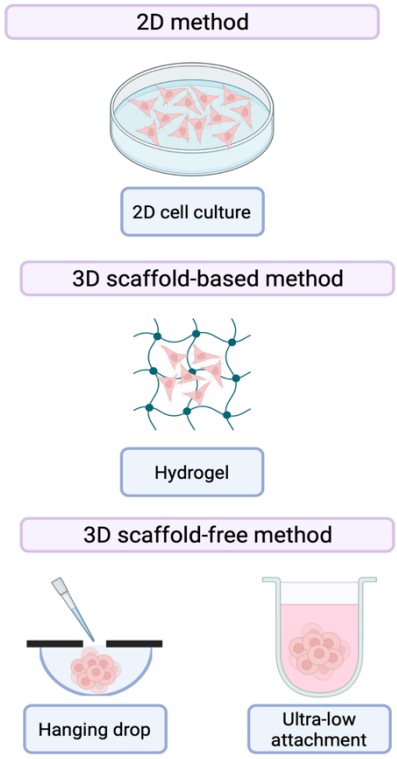

Figure 2.4 – Representation of 2D and 3D culture methods. Representation of one of the 3D scaffold-based methods, the hydrogel one and of two scaffold-free methods, the hanging drop and the usage of ultra-low attachment plates. Created in BioRender.com.

Scaffold-free techniques (**Figure 2.4**), such as hanging drop microplates, magnetic levitation and spheroid microplates with ultra-low attachment coating, show a unique feature of freely grow the 3D structures with no scaffold involved (Jensen & Teng, 2020). This approach gathers all the methods where no exogenous artificial platforms are used for promoting cell growth (Nunes et al., 2019). They promote the formation of 3D microtissues as cellular aggregates known as spheroids or multicellular spheroids that produce their own ECM (Nunes et al., 2019). The hanging drop method allows the formation of spheroids using gravity, since the spheroids hang in an open bottomless well, usually enclosed to regulate the environmental humidity of the cells (Jensen & Teng, 2020). One of the major advantages of this method is its replicability (Jensen & Teng, 2020). Magnetic levitation is performed by injecting cells with magnetic nanoparticles allowing the spheroid formation in the presence of an external magnet (Jensen & Teng, 2020). This approach allows ECM synthesis and the possible 3D culture manipulation through the external magnet, creating advanced environments, which makes it very versatile. Lastly, spheroid formation using ultra-low attachment microplates is commonly used to study tumour cells due to its simple spheroid formation by the reduction of cell adherence to the plate (Courau et al., 2019; Jensen & Teng, 2020).

More efficient drug discovery requires a better understanding of the link between cells and the ECM in which they interact, the role of growth factors and proteins in the regulation of important tumour cell processes, such as proliferation and survival (Jensen & Teng, 2020). Therefore, to predict the effectiveness of a drug on a cell, the 3D culture models better simulate the microenvironment of the tissue in which cells can proliferate, aggregate, and differentiate (Jensen & Teng, 2020). Moreover, the

3D culture models can be used to study human tissue physiology and pathophysiology *in vitro*, this culture model has been well renowned as a technology for an *in vitro* system that mimics the *in vivo* environments better than classic 2D cell culture (Costa et al., 2016; Li & Cui, 2014). Furthermore, 3D culture methods are increasingly being used in cancer research, stem cell research, drug discovery, such as for identifying and testing novel anticancer drugs, and research concerning to other types of diseases (Drost & Clevers, 2018; Jensen & Teng, 2020; Souza & C Ferreira, 2016). However, the 3D method still has some drawbacks, such as the higher cost than 2D, the need for multiple components that can make difficult the construction of the microenvironment, and the imaging in large scale of these structures (Jensen & Teng, 2020). Therefore, there is also the need for the development of adapted 3D protocols of common techniques used in 2D (Jensen & Teng, 2020).

2.4.2.1. Properties of tumour spheroids

Spheroids are micro-sized cellular aggregates that have been used to assemble models of different types of cancer *in vitro*, grown under non-scaffold methods, since they have the ability to mimic various features of solid tumours (Costa et al., 2016; Souza & C Ferreira, 2016). These structures are thought to be one of the most suitable *in vitro* model for cancer drug testing due to their ability to reproduce the cellular heterogeneity, cell-cell signalling, internal structure, gene expression and drug resistance mechanisms of the solid tumour (Souza & C Ferreira, 2016). 3D spheroids can be formed with only cancer cells or include other cell types, such as fibroblasts, endothelial cells, or immune cells, thus better mimicking the cellular diversity of the solid tumours (Costa et al., 2016).

Within the spheroids, cells can grow in close contact with each other, having the possibility to reproduce the physical interactions and the signalling pathways observed *in vivo* (Costa et al., 2016). As in solid tumours, the internal structure of the spheroids shows different layers, an external one composed of high proliferative cells, a middle one essentially formed of senescent cells, and the core that contains cells in a necrotic state (Costa et al., 2016). This layered structured is explained by the decreased presence of oxygen and nutrients in the middle layer and even more in the necrotic core, compared with the external layer (Costa et al., 2016). In solid tumours the presence of an oxygen gradient is caused by an increase in the oxygen diffusion distance due to the bigger distance between the vasculature and the cells. However, in spheroids this gradient is formed due to the higher consumption of oxygen by the proliferative cells present in the external region and because of the increase distance between the medium and the spheroid centre (Nunes et al., 2019). The resulting lack of oxygen forces the spheroids obtain energy by the conversion of pyruvate into lactate, leading to an accumulation of lactate in their interior, as is the case in solid tumours (Costa et al., 2016; Nunes et al., 2019), leadings to the acidification of the spheroid's/tumour's interior (Costa et al., 2016). This layered structure also impacts on treatment response. As discussed, drugs used in treatment show different efficacy depending on the cell cycle state of the cells, with drugs that are effective in proliferative cells having a poor effect in the interior regions of the spheroid/tumour (Costa et al., 2016). Additionally, the inside core of the spheroid cand further show more drug resistance due to the presence of an acidic interior and the fact that some of chemotherapeutics drugs require oxygen to cause damage to the tumour cells (Costa et al., 2016; Nunes et al., 2019). In addition, in the presence of lower pH, cancer cells start to express genes associated to

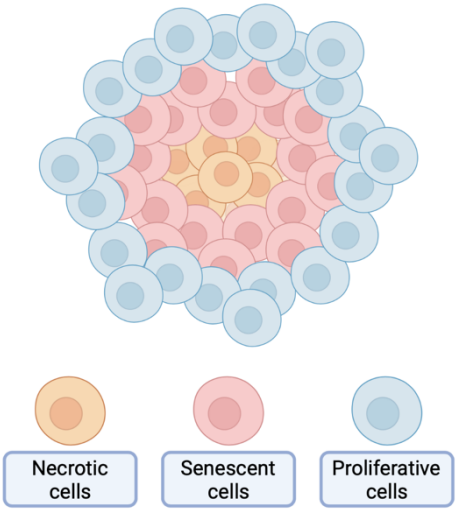

Figure 2.5 – Representation of the different layers present in the spheroids, similar to the solid tumours. Identifications of the different states of the cells within the spheroid.

hypoxia, such as HIF, leading to an enhanced proliferation and survival (Costa et al., 2016). The vascular endothelial growth factor is also highly expressed in hypoxic regions of the spheroids, being, as HIF, involved in drug resistance mechanisms (Nunes et al., 2019). The acidic pH and the lack of oxygen and nutrients induce a dormant state, senescence, on cells present in solid tumours and spheroids (Nunes et al., 2019). Several studies show that 3D structures have an increase in senescent cells than the traditional 2D cultures, presenting 58,5% of cells trapped in G0-G1 phase comparing to the 40,8%, respectively (Nunes et al., 2019). This non proliferative state within the spheroid can also be responsible for the poor therapeutic efficacy of drugs, since most of them need cellular proliferation to happen in order to have a cytotoxic effect in cells (Nunes et al., 2019).

Upon spheroid formation, the cells within start to deposit ECM noncellular constituents, such as collagen, laminin, fibronectin, and other components (Costa et al., 2016; Nunes et al., 2019). These proteins are essential to the formation of a barrier that will limit the penetration of drugs in the spheroid and limit its transport (Costa et al., 2016). Furthermore, the presence of these proteins also causes the increase in the density of the spheroid, leading to an increase of interstitial fluid pressure, and consequently an impaired penetration of used drugs (Costa et al., 2016). The gene expression profile of the tumour is also affected by its 3D structure, playing essential roles in progression, invasion and metastasis (Costa et al., 2016).

Although the fabrication of 3D spheroids constructed from different cell types is designed to try and mimic interactions between neighbouring cells and the extracellular matrix (ECM), the complex *in vivo* nature is still not matched (Nunes et al., 2019).

2.4.3. Microfluidic culture methods

Besides the fact that 3D tumour spheroid cultures are a model that mimics better the *in vivo* features of the solid tumours, it still needs some improvements and development (Jensen & Teng, 2020; S.-H. Lee et al., 2015). Therefore, technologies such as microfluidics started to be used as a tool for new *in vitro* methods in cancer research.

Microfluidics (MF) is a technology that is based on the manipulation of small volumes of fluids in a controlled way. This type of technology evolved in microfluidic devices that have high sensitivity and continuous flow (Dawson et al., 2016). The development of new cancer models using the MF devices technology is a fast-growing area of research that allows experimentation with better representation of the natural conditions of the tumour and disease (Olubajo et al., 2020). Microfluidic culture methods uses a flow rate controlled at a submillilitre scale and are able to mimic the systems and pressures of the human body with continuous perfusion, allowing the delivery of nutrients and simultaneous removal of waste (Dawson et al., 2016). Moreover, these devices conjugated with the usage of 3D cell culture models can better mimic the *in vivo* features of the solid tumours. Therefore, the introduction of spheroids into microfluidic devices makes possible the assessment of biochemical mechanisms and drug effects within the cells under more physiologically relevant conditions (Damiati et al., 2018). Furthermore, perfusion systems, such as microfluidic devices, have become a common way to replicate and monitor *in vivo* environments (Jensen & Teng, 2020). They offer an innovative method for studying the *in vivo* environment, for cell proliferation and chemosensitivity of anti-cancer drugs assays in a real-time manner. (Dawson et al., 2016; Jensen & Teng, 2020).

The microfluidic devices also allow the integration of patient tissues, allowing the effect of various drug combinations and chemical reactions to be monitored and assessed with the potential of identifying optimal treatment strategies prior to the first administration in the patient (Dawson et al., 2016; Olubajo

et al., 2020). Since the first evidence of microfluidic culture of rat brain tissue slices in 2003, various devices have been designed and utilised for the culture of both animal and human tissue under *ex vivo* conditions, showing the different applications that can have (Dawson et al., 2016). Besides the impact that microfluidics made on science, this type of technology still requires a range of subsystems and components with the integration of complete systems (Dawson et al., 2016). Furthermore, the microfluidic system models still need some improvement since some of the challenges are: the fragility of the models, the complexity of the systems that can be interrupted by the presence of a single bubble in the chamber, and the limitation in long-term experiments using common media (Jensen & Teng, 2020). However, the ability that these devices have to integrate a lot of parameters is a step towards the development of personalised medicine and a robust methodology for screening drug effects (Dawson et al., 2016).

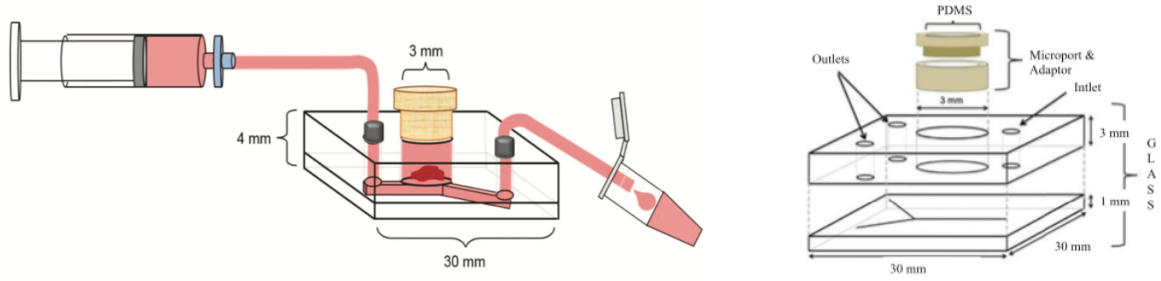

Figure 2.6 - Schematic of the microfluidic design and setup maintained at 37°C with constant media influx and simultaneous removal of waste products. Adapted from Dawson, A., Greenman, J., Bower, R., & Green, V. (2016). Microfluidics: the fur-free way towards personalized medicine in cancer therapy. *Drug target review*, 3(1), 12-17.

2.5. Aims

Although the knowledge for cancer treatment has increased substantially, it still is a huge worldwide health problem, with this disease still being the second leading cause of death globally (Drost & Clevers, 2018; Neufeld et al., 2021). Therefore, the development of new and targeted therapies is essential since it can lead to preventive and personalized therapies which can reduce the number of cancer deaths (Drost & Clevers, 2018). One of the main challenges in drug development is the translation of scientific knowledge from the lab bench to patient treatment (Drost & Clevers, 2018). This is mainly caused by the fact that most cancer models poorly reflect the patient's tumour features *in vivo*, leading to many drugs failing in pre-clinical trials (Drost & Clevers, 2018). The usual preclinical drug development process relies on the *in vitro* evaluation of drug toxicity/efficacy in 2D cell culture followed by animal studies (Neufeld et al., 2021). Although this type of traditional cell culture has tremendous value in biomedical research and in drug screening, since it is very low cost and easy to use, it does not mimic the tissue-specific architecture and the presence of nutrients and oxygen gradients (Neufeld et al., 2021; Nunes et al., 2019). Therefore, new and improved *in vitro* models have been developed with the aim of reproducing more closely the features of *in vivo* human tumours, improving the drug development pipeline (Nunes et al., 2019). 3D culture methods represent relevant biological aspects of the *in vivo* structures, since they mimic structural organization, cell-cell interactions, and cell-extracellular matrix interactions (Neufeld et al., 2021; Souza & C Ferreira, 2016). Furthermore, the usage of these types of models, spheroids and organoids, increase the relevance and efficiency of *in vitro* studies and reduce the dependence of the *in vivo* ones, leading to better drug candidates for clinical trials (Souza & C Ferreira, 2016). Although the 3D models have shown great promise, they often do not reflect all the complexity of tumours *in vivo*, as they lack the functional blood vessels (Neufeld et al., 2021). The development of new cancer models using the MF devices technology is a fast-growing area of research that allows

experimentation with better representation of the natural conditions of the tumour and disease (Olubajo et al., 2020). Microfluidic culture methods allow the mimic of the fluids' pressures of the human body with continuous perfusion, with the maintenance of the 3D cell structure of the spheroids culture models which can better mimic the *in vivo* features of the solid tumours.

Currently it is possible to find many studies in colorectal cancer and glioblastoma that are starting to test the applicability of 3D culture methods in drug resistance and tumour mechanisms research. Most of the studies make a comparison between the traditional 2D culture method and a chosen 3D method upon commonly used treatment by assessing key features of specific cancer molecular mechanisms (Chen et al., 2020; Lee et al., 2015; Lv et al., 2016; Musah-Eroje & Watson, 2019). However, most of them use different types of 3D cell culture methods, such as the usage of different cell lines, the presence or not of a scaffold, and the presence or not of different types of cells important in the tumour development. Furthermore, studies comparing the three cell culture methods, 2D, 3D static and 3D microfluidic, as this following study, are still lacking. Although some of these studies show some evidence that the 3D culture methods can be similar to the *in vivo* tumour's behaviour, this type of cell culture methods are still recent and in need of more deep analysis.

The present work was developed as a part of an ongoing collaboration between the Gama-Carvalho and Greenman group, at the University of Hull, who have been developing simple microfluidic systems for growing tumour cells. The main goal of this work was to compare how growing tumour cells as monolayers (2D culture), as 3D spheroids, and as 3D spheroid within a microfluidic device, influences the effectiveness of chemotherapeutic agents. For this purpose, we used as a model the HCT-116 colorectal cancer cell line and the U87 MG glioblastoma cell line, treated with 5-fluoracil or temozolomide, respectively. To assess the cellular responses to these chemotherapeutic agents, the following specific aims were defined:

- Establishment of the 3D spheroid and 3D spheroid microfluidic device cell culture methods for both cell lines (originally planned to be performed at the Greenman lab).

- Establishment of methods to characterize the cellular response to drugs, focusing on cell viability, expression of key gene markers, cellular proliferation and spatial organization of the cells.

- Characterization of the response of HCT-116 and U87 MG cells grown under the three different culture methods to the presence or absence of the chemotherapeutic agents 5-fluoracil and temozolomide, respectively.

This systematic approach provides critical insights on the impact that different culture conditions have on drug screening protocols, providing valuable information for the implementation of cost-effective methods that can better mimic the responses observed in patients.

3. Materials and Methods

3.1. Cell Culture

HCT-116 cells (kindly gifted by Dra. Luísa Romão, INSA) were cultured in McCoy's 5A medium (McCoy's 5A 1X with L-Glutamine, Corning, USA) supplemented with 10% (v/v) fetal bovine serum (FBS, Biowest). U87 MG cells (kindly gifted by Dra. Cristina Carvalho, Faculty of Farmacy) were cultured in Eagle's Minimum Essential Medium (MEM, Corning, USA) supplemented with 10% (v/v) fetal bovine serum (FBS, Biowest). Both cell lines were grown in a cell culture incubator at 37ºC with 5% CO_2.

3.1.1. 2D Cell Culture Method

For the 2D cell culture method, the cells maintained in culture with a passage every two days with a dilution of 1:2 and 1:6 during the weekly days, and a 1:4 and 1:8 dilution during the weekend, for the U87 MG and the HCT-116 cell lines, respectively. The passage frequency was determined by the flask's confluency being between 70-80 %. The cells were seeded in a 96-well flat plate (Labbox Labware, Spain) at the following cell densities: 12.500 cells/mL for the HCT-116 cell line and 25.000 cells/mL for the U87 MG cell line. The first and last column and row of the 96-well plate were loaded with sterile PBS 1X (Fisher Bioreagents, EUA) to avoid evaporation and not used for cell seeding. The other 96-well plate wells were loaded with 200uL of cell suspension. The plates were kept at 37ºC with 5% CO_2 for 3 days.

3.1.2. 3D Cell Culture Method

Spheroids were formed from both cell lines in Ultra-Low Attachment 96-well plates (ULA, Corning, USA) following as starting point the protocol from Greeman Lab: loading of the wells of the 96-well plate with 200uL of cell suspension containing 20.000 cells (100.000 cells/mL) and incubate them for 3 days at 37ºC with 5% CO_2. The cells were culture in monolayer as described above. After protocol optimization for both cell lines, the cells were seeded in an Ultra-Low Attachment 96-well plate as followed: HCT-116 with a cell density of 12.500 cells/mL and U87 MG with a cell density of 100.000 cells/mL. From this solution, 200µL were added to the central wells of the 96-well ULA plate. The first and last column and row of the 96-well plate were loaded with sterile PBS 1X (Fisher Bioreagents, EUA) to avoid evaporation and not used for cell seeding. The plates were kept at 37ºC with 5% CO_2 for 3 days to allow the formation of the spheroids.

3.2. MTS Assay

To quantify cell viability, the CellTiter 96 Aqueous One Solution Cell Proliferation Assay was used. After optimization of the assay protocol for each cell line, it was performed as follow. The cells were seeded into a 96 well plate, according to the cell culture method used, and incubated for 3 days in the protocol optimization experiments and for 5 days for the treatment experiments. Control wells for the treatments were also performed. Half of the medium present in the plate wells were taken and a volume of 20uL of the MTS reagent was added to each well and incubated at 37ºC with 5% of CO_2 for two hours. After the metabolization of the MTS by the cells, the absorbance values of the seeded wells, control wells and blank wells were measured at 495nm using the plate reader Victor 3V (Perkin-Elmer).

3.3. RNA Extraction and Integrity Assessment

Total RNA was extracted from HCT-116 and U87 MG cell line using TRIzol (Zymo Research) reagent for both cell culture methods. For the 2D cell culture method, 50uL of TRIzol reagent was added to each well and mixed well until all the cells were detached, and the cell suspension from 4 wells was collected into an Eppendorf tube for RNA isolation and purification. For the 3D cell culture method, the same procedure was followed but the mechanical disruption of the spheroids into the reagent was performed in an Eppendorf tube. The RNA isolation was done according to the manufacturer's instructions.

The RNA extracted from samples of the experiments with the chemotherapeutic drugs followed the same TRIzol reagent protocol, but the RNA isolation was done using the Direct-zol RNA Miniprep kit (Direct-zol RNA Miniprep kit 50 preps, Zymo, CA, USA) following the manufacturer's protocol.

3.4. Reverse Transcription and PCR

The cDNA synthesis was performed using Reverse Transcriptase (RT, NZYTech, Portugal) using the OligodT (Nzytech, Portugal) priming method, according to the manufacturer's protocol. This synthesis was performed using the same input of total RNA in each sample, being this value determined by the higher input of RNA possible for the sample with the lowest RNA concentration.

PCR was performed using a 1:10 dilution of the synthetized cDNA and the NZYTaq II DNA polymerase (NZYTech, Portugal) according to the manufacturer's protocol, with a total reaction volume of 25uL and specific primers for the target genes (**Table 3.1**).The thermocycler conditions used were 90ºC for 3 minutes, followed by 35 cycles of 94ºC for 30 seconds, 55ºC for 30 seconds and 72ºC for 30 seconds, and 8 minutes at 72ºC. These conditions were used for each gene target, except the actin that was performed using 1 minute of incubation for each temperature of the 35 cycles. The PCR products were analysed by electrophoresis on 2% agarose gels using a voltage of 90V/100V.

3.5. qRT-PCR – Real Time PCR

The real time q-RT-PCR was performed in Bio-Rad CFX96 qPCR, using NZYSpeedy qPCR Green Master Mix 2x (NZYTech, Portugal) according to the manufacturer's protocol. The cDNA samples were diluted 1:4 and a total reaction volume of 25uL was used and specific primers for the target genes **(Table 3.1**). The qRT-PCR analysis was performed using the ΔΔCt method for quantification and the HPRT1 gene as the internal control gene.

Table 3.1 - Sequence of the primers used in this project (5'→3').

Gene Target	Forward	Reverse
Actin	GAAAATCTGGCACCACACCT	GGCCGGACTCGTCATACTC
CDKN1A	GGCAGACCAGCATGACAGATT	AAGGCAGAAGATGTAGAGCGG
cMyc	CTTACAACACCCGAGCAAGG	GTCGCAGTAGAAATACGGCT
GADD45A	TCAACGTCGACCCCGATAA	GATGTTGATGTCGTTCTCGCA
HPRT1	TGACACTGGCAAAACAATGCA	GGTCCTTTTCACCAGCAAGCT

3.6. Immunofluorescence

3.6.1. 2D Cultures

The cells were seeded in Greiner 96-well flat bottom black polystryrene wells plate (CellStar, Sigma, USA) following the 2D cell culture model protocol. The cells were quickly washed with PBS without agitation, fixed using a solution of 3,7% formaldehyde in 1x PBS for 10 minutes, followed by three PBS washes of 5 minutes. The permeabilization was done using a 0,5% TritonX-100 solution in 1x PBS for 10 minutes, followed by three PBS washes of 5 minutes. Before the addition of the primary antibody, the cells were washed with a 0,05% Tween-20 solution in 1x PBS. 4uL of the Ki-67 primary antibody (eBioscience, ThermoFisher, EUA) with a dilution of 1:100 in a PBS-Tween solution, was added to the cells and incubated for 1h at room temperature in a humid chamber. Three washed of 5 minutes each with PBS-Tween solution were performed. Subsequently, 4uL of a solution with the Alexa 488 anti-rat secondary antibody (Molecular Probes, EUA) and rhodamine phalloidin (Abcam, UK) staining, both with a dilution of 1:1000 in a PBS-Tween solution, was added and incubated for 30 minutes at room temperature in a humid dark chamber. The cells were washed three times for 5 minutes with PBS-Tween solution and the DNA staining with Hoechst (Sigma-Aldrich, EUA) at a concentration of 1µg/mL in PBS 1X. The cells were maintained in PBS 1X and kept at 4ºC hidden from the light. The images were captured using the widefield system DMI6000B (Leica Microsystems) and the images were analyzed using Fiji and CellProfiler software.

3.6.2. 3D Cultures

3.6.2.1. Cryopreservation of spheroids

To perform immunohistochemistry in the spheroids, it was necessary to cryopreserve them first. After protocol optimization, 4 to 6 spheroids, from the same cell line and with the same treatment, were collected to a glass tube, the medium was removed, and they were washed with PBS 1X. Spheroids were fixed overnight at 4ºC in 1% FISH solution. The spheroids were washed with PBS 1X and incubated for 5/6 hours at 4ºC in T1 solution (**Table 3.2**). Following this step, the spheroids were placed into a 4-well plate, previously greased with vaseline to help its removal later, and incubated overnight at 4ºC in T2 solution (**Table 3.2**). The following day the spheroids were incubated in T3 solution (**Table 3.2**) for 1 hour in a 37ºC water bath, followed by an 1hour incubation at 4ºC. The spheroids embedded in gelatin were cut in cubes and frozen using isopropanol and dry ice. The spheroids were kept at -80ºC.

Table 3.2 – Description of the composition of the solutions used for the cryopreservation of the spheroids.

Solutions	Composition
FISH	0,12M phosphate buffer with 4% sucrose and 1% paraformaldehyde
Solution T1	0,12M phosphate buffer with 4% sucrose
Solution T2	0.12M phosphate buffer with 15% sucrose
Solution T3	0,12M phosphate buffer with 15% sucrose and 7,5% gelatin

3.6.2.2. Spheroids cuts and immunofluorescence

Before the immunofluorescence protocol was performed, the previously frozen spheroids were cut in 7µm slices using the CM1860 UV Cryostat (Leica Microsystems).

For the immunofluorescence protocol the cuts were placed on microscopy glass slides and washed three times with PBS 1X for 5 minutes. Following this step, an incubation of 15 minutes in Triton 0,1% solution was used for spheroid's permeabilization, flowed by three 5 minutes PBS 1X washes. A 1:10

NGS solution in 1% PBS/BSA was used for 30 minutes sample blocking. The Ki67 primary antibody (eBioscience, ThermoFisher, EUA), with a dilution of 1:100 in a PBS-Tween solution, was incubated over night at room temperature in a humid chamber. Following the next day, three 5 minutes PBS 1X washes were performed and a solution with the Alexa 488 anti-rat secondary antibody (Molecular Probes, EUA) and rhodamine phalloidin (Abcam, UK) staining, both with a dilution of 1:1000 in a PBS-Tween solution, was incubated for two and half hours at room temperature in a humid dark chamber. Following, three 5 minutes PBS 1X washes were executed and the slides were incubated with DAPI staining for one minute, followed by a single PBS 4X wash. Three 5 minutes 1X PBS washes were performed, and the microscopy glass coverslips added to the microscopy slides with a drop of mounting media and sealed. The microscopy preparations were kept at 4ºC in the dark and visualized using the BclX60 microscopy (Olympus) and analyzed using the Fiji software.

3.7. Chemotherapeutic Drugs Treatment

For the 5 days chemotherapeutic drug treatment two different drugs were used, 5-fluorouracil (Sigma-Aldrich, USA) and temozolomide (TCI Europe), for the treatment of HCT-116 cell line and the U87 MG, respectively. The drug stock solutions were previously prepared in DMSO with a concentration of 10mg/mL each and maintained at -80ºC. Both drug solutions were diluted in medium with a final concentration of 500µM for usage in the cell's treatment, being these solutions freshly prepared for each experiment and kept at 4ºC. A 100µM sodium azide solution was used as a positive control for cell death, freshly prepared from a 5M sodium azide, and a 500µM DMSO solution as a negative control. The cells were seeded as described before for each cell culture method and cell line. After the 3 incubation days, half of the medium from each well was taken and replaced by the same amount of two times higher concentration of drug medium, and the same for the control wells. During the treatment period, the medium was changed every 2-3 days, by replacing half of the medium volume with new one with the desired drug concentration. The experiments for each cell culture model were all done at the same time in the same day for each biological replicate.

4. Results

4.1. System and protocol validation

The 3D methods proposed in this work were planned to be done in Greenman Lab, but due to the Covid-19 pandemics this was not possible. Therefore, the spheroid formation method and the microfluidic device culture method had to be stablished in our lab. Moreover, the cell number used for the spheroid formation protocol had also to be adjusted to each performed assay and used cell line.

4.1.1. Spheroid formation optimization

The first step of this project was to optimize the spheroid formation protocol in the lab. In order to do this, the Greenman Lab spheroid formation protocol was used as the guideline for the spheroid formation for both cell lines used. Therefore, to assess the spheroid formation during the 3 incubation days in culture, HCT-116 and U87 MG cells were seeded at 100.000 cells/mL, which was the recommended density described in Greenman Lab protocol. During the spheroid formation period, the wells were photographed in order to follow their behaviour and determine their features, as shown in **Figure 4.1**.

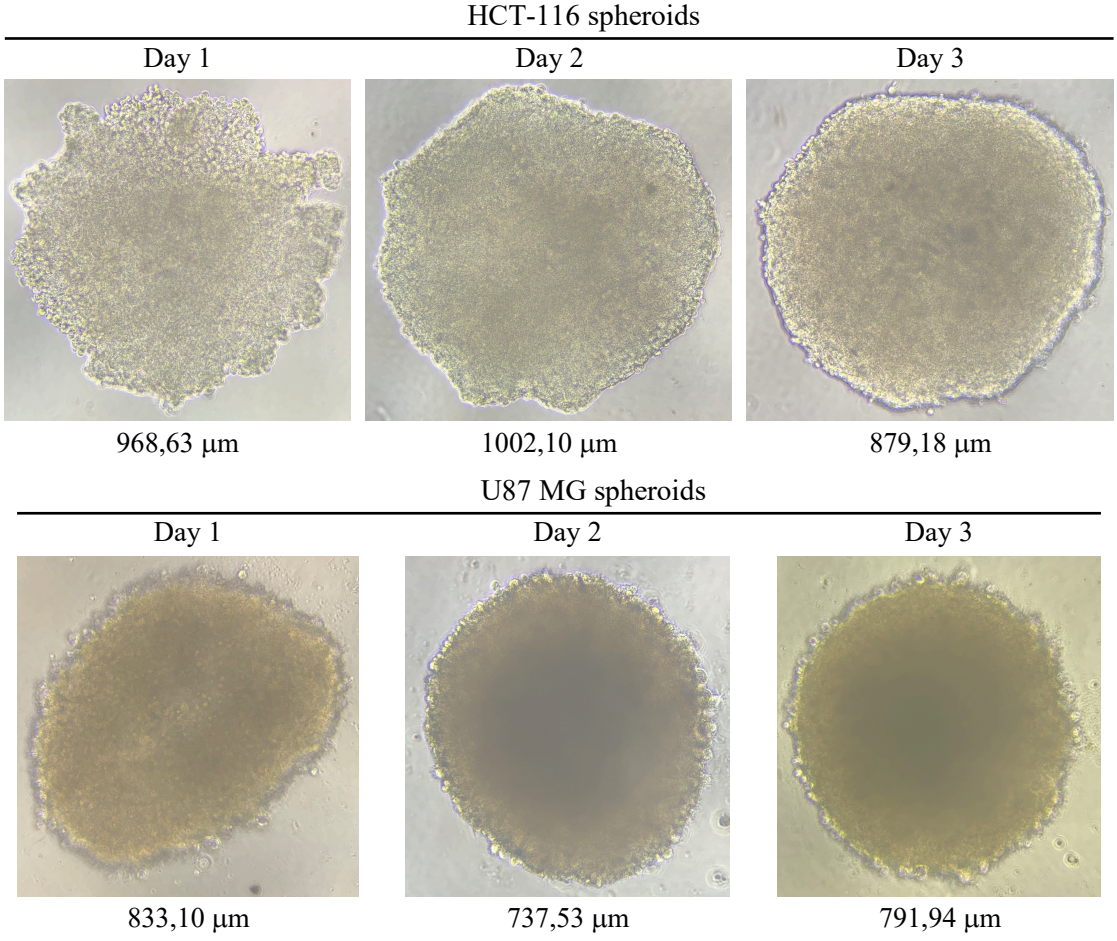

Figure 4.1 – Representation of spheroids from HCT-116 and U87 MG cell lines. Both cell lines were seeded at 100.000 cells/mL in each well of the ULA plate and kept in the cell incubator for 3 days. The day zero is the day of the seeding. The biggest diameter (Feret distance) is represented bellow each image and was calculated using the Fiji software.

This experiment showed that the spheroids were formed correctly and theirs shapes changed during the 3 days formation towards a more circular shape present at the 3rd day. The spheroids' diameter also changes during their formation showing a decrease from the 1st day until the 3rd day, which can possible be explained by the formation of a more compact structure in the end of the incubation time. After the cell number optimization for the spheroid formation performed for each assay, the formed spheroids were again photographed at the last day of incubation and their diameter measured, as showed in **Figure 4.2**.

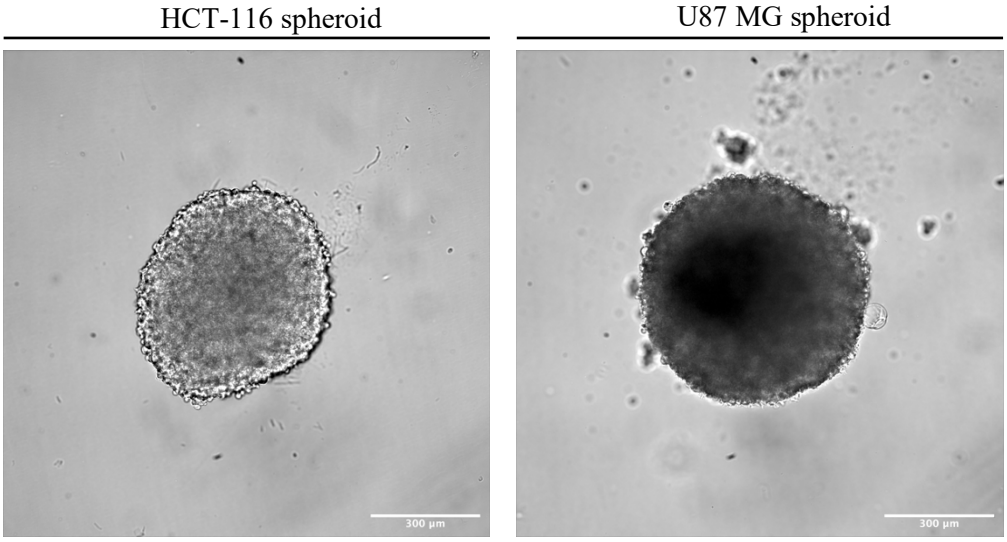

Figure 4.2 - Representation of spheroids from HCT-116 and U87 MG cell lines. The HCT-116 cell line was seeded at 12.500 cells/mL and the U87 MG cell line was seeded at 100.000 cells/mL in each well of the ULA plate and kept in the cell incubator for 3 days. The day zero is the day of the seeding. The biggest diameter (Feret distance) is represented bellow each image and was calculated using the software Fiji.

As the cell number used at the seeding for the spheroid formation of each cell line was different it is possible to obverse a denser and more compact spheroid formed from the U87 MG cell line in comparison to the ones from HCT-116 cell line.

4.1.2. Microfluidic device set up and optimization

Besides the 2D and 3D static cell culture models, the two cell lines were also cultured using a microfluidic device developed by Greenman Lab. However, the possibility of me going to Greenman Lab to do this part of the work there and benefit from their expertise was cancelled due to Covid-19 pandemics. Therefore, the microfluidic device and the necessary material was sent to our lab and online tutoring about its usage was provided. Furthermore, it was necessary to set up all the components and adapt them to the existing material, in order to put the device working. The first step was connecting every component and starting to understand how it worked. This microfluidic device is based on a very simple rational, which is the entry of culture medium into a tube connected with the device, the insertion of the spheroids previously cultured in the 3D static model, and the outflow of the medium through another tube, showed in **Figure 4.3**.

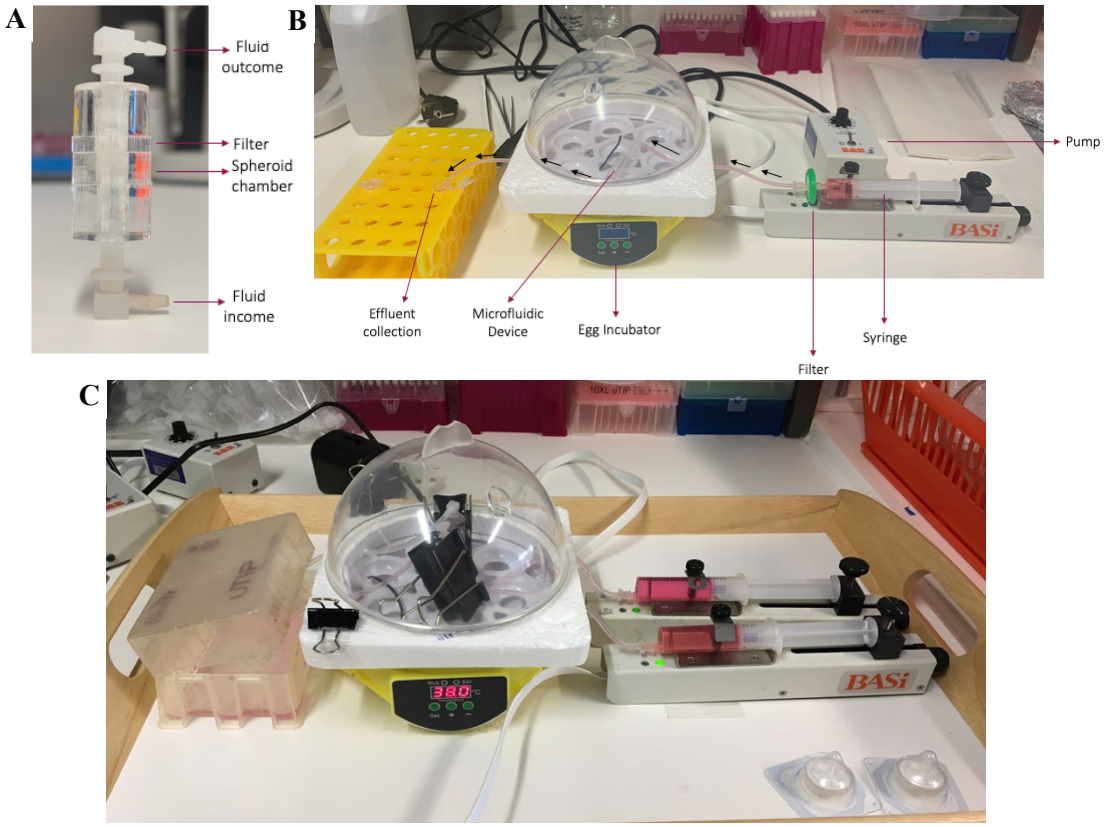

Figure 4.3 - Representation of the microfluidic components and set up. (A) The microfluidic device and main constituents. **(B)** Working flow of the culture medium within the device and all the components involved in the device and set up. **(C)** Representation of the device final set up.

The flow rate of the device is set up in the pumps connected to the device's tubes and its of extreme importance for the maintenance of the spheroids' integrity. Therefore, the second step was the calibration of the devices, in which the flow rate should be between 2 and 6µL/min. To achieve this aim, the culture medium was loaded into the syringes and different pump flow rates were tested and the outflow medium measured. Furthermore, the conclusion of these experiments was that the pump's flow rate were approximately 10 times slower than the actual flow rate in the device. Therefore, this made sense, since the pumps were manufactured for syringes filled with 1mL of medium, and the syringes used were loaded with 10mL of medium. For instance, for a flow rate of 5µL/min in the device, the pump's flow rate was set up at 0,5µL/min.

Besides the importance of the setting up the correct flow rate, the avoidance of bubbles inside the device chamber was also of extreme importance since they could disrupt the spheroid's 3D structure along the media's flowthrough. This was one of the bigger issues to avoid, since it is necessary to load every component of the device with media prior to the insertion of the spheroid, and for its insertion it is needed to open the device, which makes it difficult to avoid the formation of bubbles. Therefore, it was necessary to test a lot of different approaches spatial set ups and the crucial help from Dr. John and his PhD students in order to solve this technical problem.

The last step was to test culture the spheroids using the optimized set up (**Figure 4.3**). Since the cell's treatment was for 5 days, although this first experiment was only using normal medium, the cells were kept for the same amount of days. It was possible to perform the assay during the 5 days, however at the last day the media started to seem contaminated. Due to cell culture facility availability, it was

necessary to transport all the set up to the cell culture room to refill the syringes and then maintain it in the lab bench for the rest of the time. Therefore, although every component was disinfected every time it was in cell culture, due to the number of components and the absence of antibiotics in the medium, it was not possible to avoid contamination. Furthermore, due to time limits and the fact that every result from the two other culture models were performed without antibiotics, it was not possible to perform any of the analysis assays to the spheroids cultured in the microfluidic device.

4.1.3. Viability assay

The chosen assay to assess the cell viability of the cells cultured in all three cell culture methods was the MTS assay. This protocol consists in a colorimetric method used for the relative quantification of the viable cells that is not harmful for cells and it is very simple to perform.

Although this is a simple assay to perform, it has some parameters that must be established to each used cell line. This method is done in a 96-well plate and the number of cells seeded in each well is dependent of the cell line. Additionally, the MTS incubation time is also variable from 1 to 4 hours depending on the formation of the coloured formazan product by each cell line. For this reason, the first step was to assess the number of cells that should be seeded per well and the reagent incubation time, for each cell line used only for the well-established 2D cell culture condition. Having in consideration the number of cells and incubation time mentioned in the product sheet, the following conditions were tested: 50.000, 100.000 and 400.000 cells/well, for 1, 2 and 4 hours of incubation with MTS reagent. The results obtained for this assay are represented above in **Figure 4.4**.

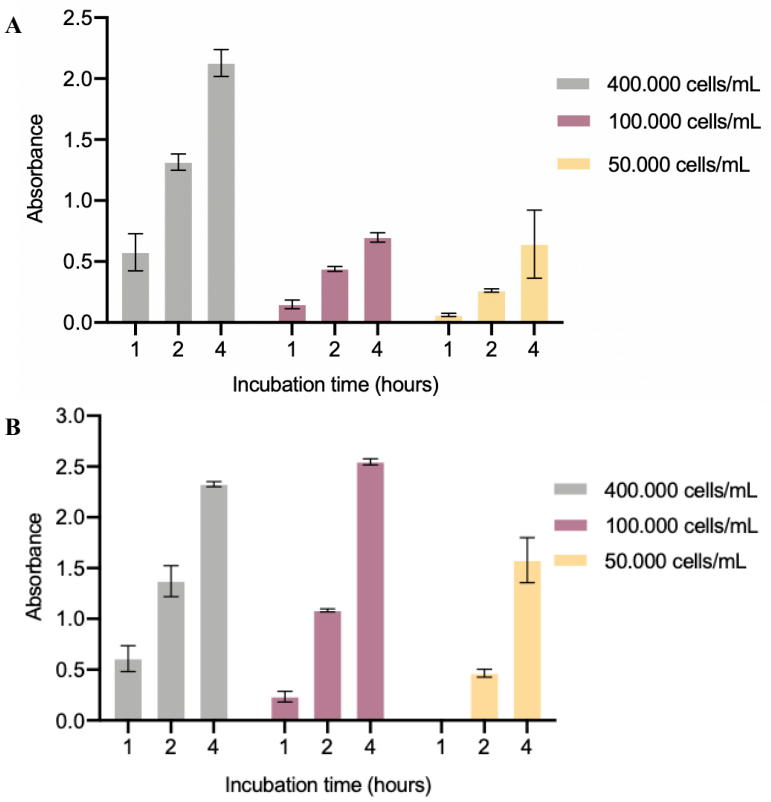

Figure 4.4 - MTS assay conditions validation for 2D cell culture model. The cells were seeded at each cell concentration for 24 hours prior to the MTS assay. Data is presented as a mean of three technical replicates with the standard deviation. **(A)** HCT-116 cell line. **(B)** U87MG cell line.

By the analysis of the **Figure 4.4** and having in consideration that the absorbance should not be higher than 1.0, the best conditions for the HCT-116 cell line are between 50.000 and 100.000 cells/well

with an incubation time between 1 to 2 hours. For the U87 MG cell line the cell density for the seeding should also be within that range, but with an incubation time of 2 hours.

Having established the assay's best conditions for the 2D cell culture model, the next goal was to determine the best conditions for the 3D cell culture method, since this assay was not a 3D specific protocol. Therefore, the conditions tested for the 3D experiment had in consideration the best conditions observed in the 2D assay and the number of cells followed in the Greenman Lab protocol to produce U87 MG spheroids. The results obtained are shown below in **Figure 4.5**.

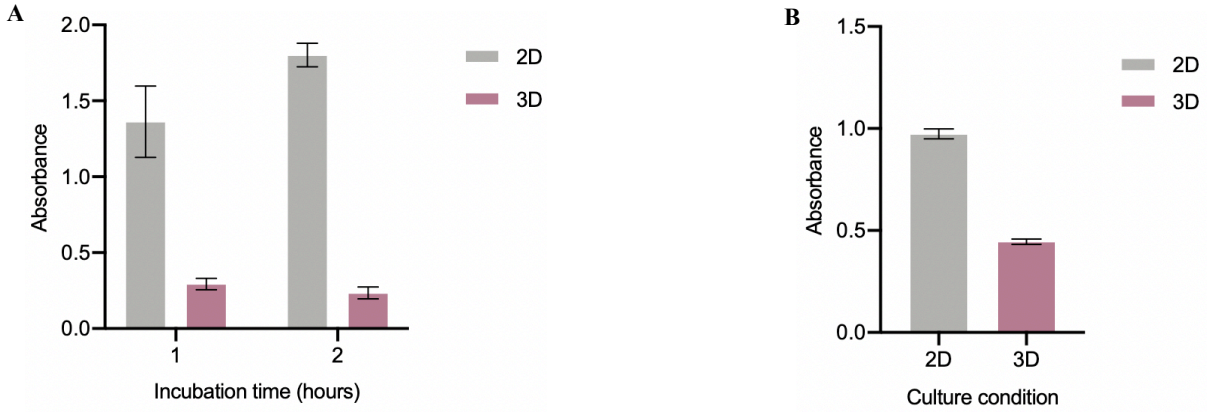

Figure 4.5 - MTS assay conditions validation for 3D cell culture model. The cells were seeded at 20.000 cells/well for 3 days for each cell culture model and cell line, prior to the MTS assay. Data is presented as a mean of three technical replicates with the standard deviation**. (A)** HCT-116 cell line. **(B)** U87MG cell line, with 2 hours of MTS reagent incubation time.

By the analysis of **Figure 4.5**, for the HCT-116 cell line there is no difference between the absorbance values for 1 and 2 hours of MTS incubation for the 3D culture method, which means that for this cell culture method the assay could not be working. For these reasons, to make sure the MTS assay was working properly, a new 2D assay using sodium azide was performed to prove that the MTS assay was, in fact, assessing the cell viability (**Figure 4.6**). Therefore, the absorbance value obtained in the treated wells was expected to be lower than the one of the control cells, since the sodium azide would kill the cells and, for that reason, the cell viability should be lower. Thereafter, with this assay the best conditions for the 3D experiment could be chosen.

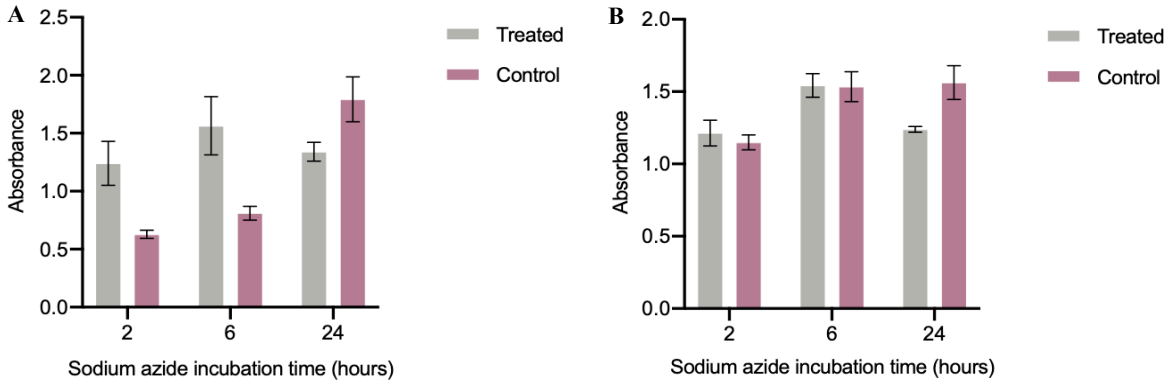

Figure 4.6 - MTS assay for 2D experiment with sodium azide at a concentration of 10mM. The cells were seeded at 20.000 cells/well 24 hours prior to the addition of sodium azide treatment. The MTS reagent was incubated for 2 hours. Data is presented as a mean of three technical replicates with the standard deviation**. (A)** HCT-116 cell line. **(B)** U87MG cell line.

Since the results obtained in **Figure 4.6** show a small difference between the absorbance values of the treated wells and the control ones, it was decided that the sodium azide concentration should be higher and with a longer exposure time. Having this in consideration, a new assay was performed for the two types of cell culture models (**Figure 4.7**).

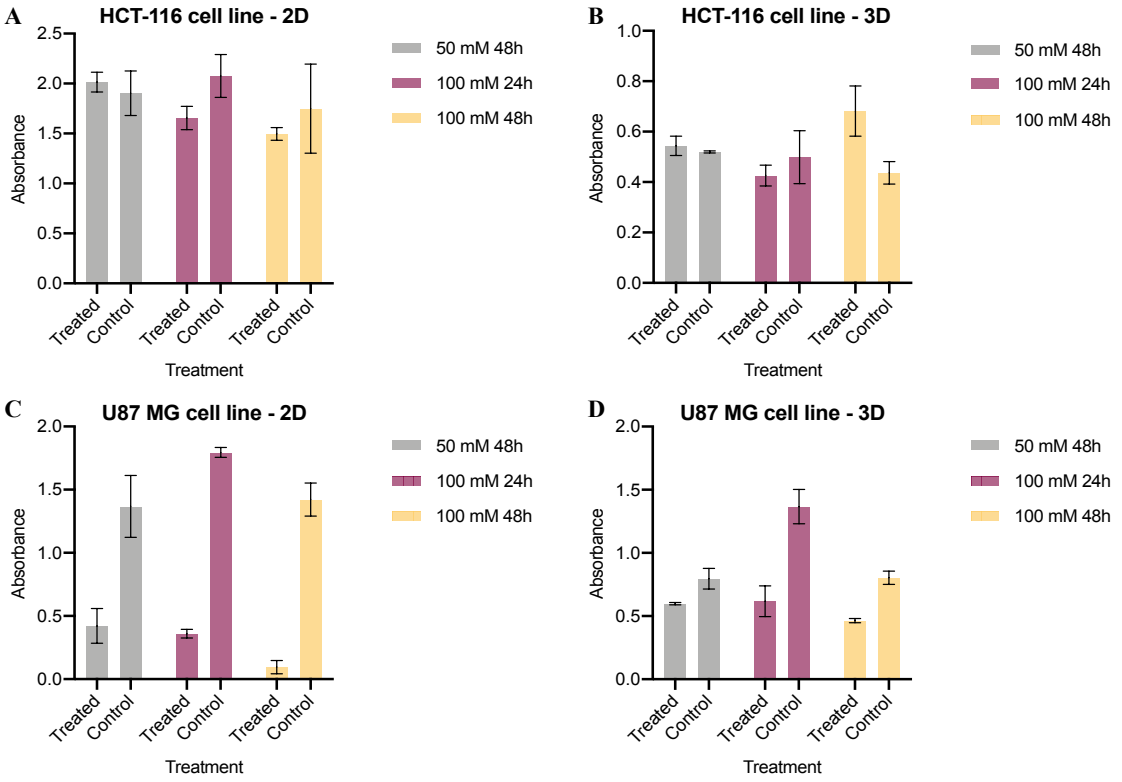

Figure 4.7 - MTS assay for 2D and 3D cell culture models experiment with sodium azide. For the 2D experiment the cells were seeded at 20.000 cells/well 24 hours prior to the addition of sodium azide treatment. For the 3D experiment the cells were seeded at the same density but for three days to allow the formation of the spheroids. The MTS reagent was incubated for 2 hours. Data is presented as a mean of three technical replicates with the standard deviation**. (A)** HCT-116 cell line 2D method, **(B)** HCT-116 cell line 3D method, **(C)** U87MG cell line 2D method, **(D)** U87MG cell line 3D method.

By the analysis of **Figure 4.7**, for the HCT-116 cell line the difference between the treated and control wells is not significant, independent of the treatment used. However, that is not observed for the U87 MG cell line, in which a significant difference between the control and treated wells is observed, besides the lower absorbance values obtained for the 3D condition in comparison to the 2D. Therefore, since the HCT-116 cell line has a faster growth than the U87 MG, approximately 2,5 times faster, the seeding cell number was thought to be the reason for the insignificant differences of cell viability in the HCT-116 cell line with and without sodium azide treatment. Moreover, a new assay with the number of cells seeded adjusted to each cell line growth was performed and the seeding time for both culture methods (**Figure 4.8**).

From the results (**Figure 4.8)** it is possible to determine the best culture conditions for each cell line and for each culture method for the MTS assay. Furthermore, the MTS assay was proven to be working properly as a measure of cell viability. Therefore, this assay can now be used as measure of cell viability in the experiments using chemotherapeutic drug treatment.

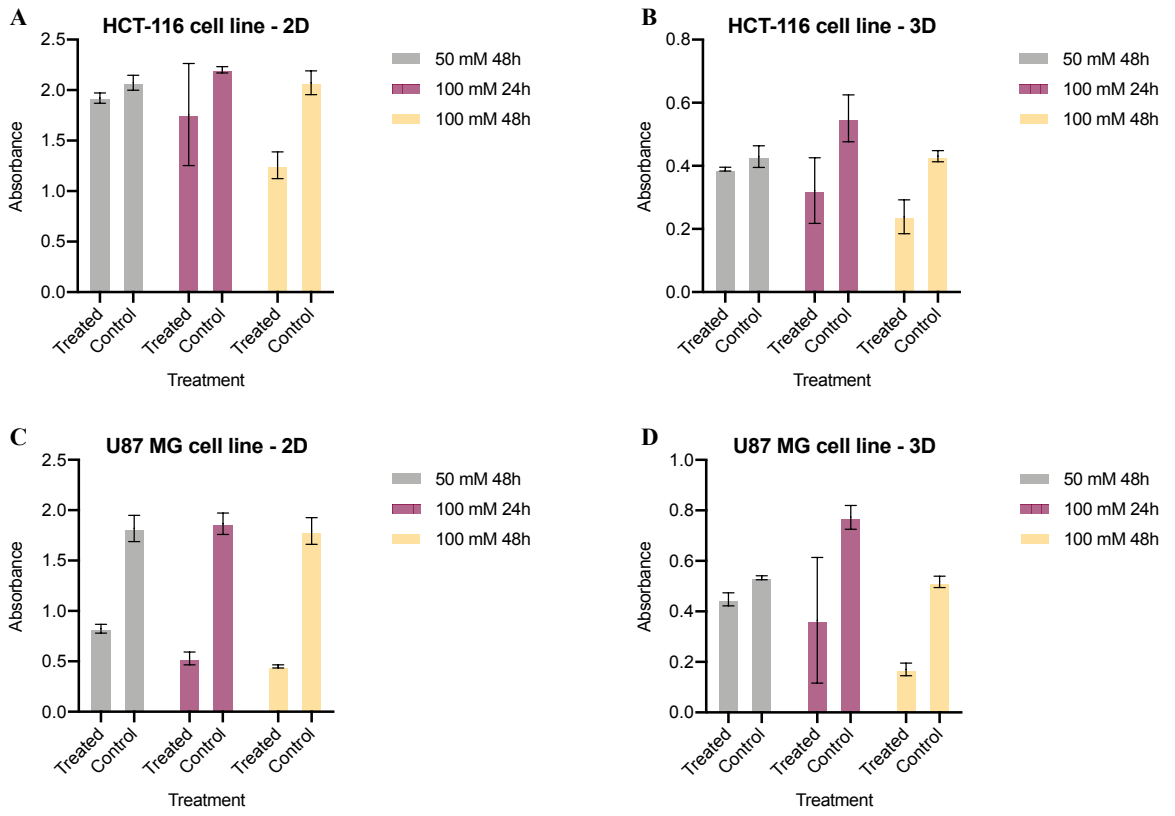

Figure 4.8 - MTS assay for 2D and 3D cell culture models experiment with sodium azide. For the HCT-116 cell line the cells were seeded at 2.500 cells/well for both cell culture methods. For the U87MG cell line the cells were seeded at 5.000 cells/well for the 2D method and at 20.000 cells/well for the 3D method. In both cell culture methods, the cells were seeded for three days. The MTS reagent was incubated for 2 hours. Data is presented as a mean of three technical replicates with the standard deviation**. (A)** HCT-116 cell line 2D method, **(B)** HCT-116 cell line 3D method, **(C)** U87MG cell line 2D method, **(D)** U87MG cell line 3D method.

4.1.4. Gene Expression Assessment

With the aim of assessing the differences in gene expression upon chemotherapeutic drug treatment, firstly the amount of spheroid material needed for difference in gene expression detection had to be determined. For this goal, the first step was testing the amount of RNA material that was necessary to detect housekeeping genes by RT-PCR for both cell culture models, without any treatment. To do this we started with total RNA isolated from 1 or 4 wells of a 96-well plate and the following targets genes: actin, HPRT1 and GADD45A. The HPRT1 gene it is a housekeeping gene very use in quantitative RT-PCR, which was the technique that it would be used for assessing the differences in gene expression upon treatment, therefore important to be detected. The GADD45A gene is involved in DNA damage repair, cell cycle and apoptosis in the response to physiological or environmental stress (Liu et al., 2018). Therefore, it was expected that its expression was low and for this reason could be used as a low expressed gene to assess if it was possible to identify low expressed genes with the amount of material used. The results from this experiment are represented in **Figure 4.9**.

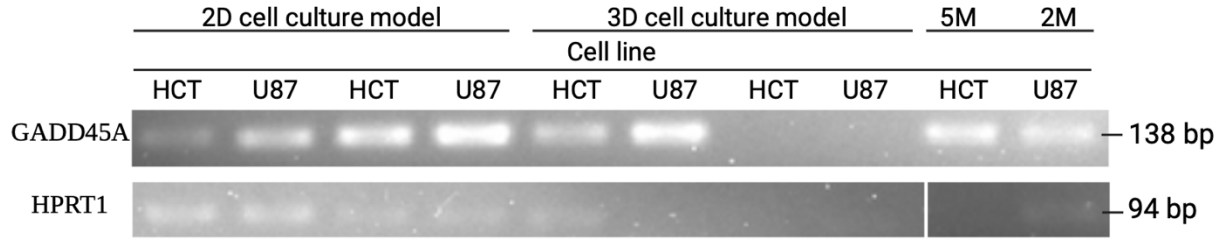

Figure 4.9 - Representation of the PCR products in a 2% agarose gel. The legend for each well contains the gene assessed, the amount for biological material used, the cell culture method and the cell line, respectively. The wells that contain as the amount of material T75 are the positive controls, in which it was used enough cells to detect any gene. HCT - HCT-116 cell line, U87 - U87 MG cell line.

From this experiment, the wells from samples collected from 4 wells were expected to have more intense bands than the wells from samples collected from 1 well, since the amount of material was higher. However, by the analysis of the results (**Figure 4.9**), this do not happen for every sample. Besides this, all the wells loaded with PCR samples specific for the actin gene are clear, meaning that something wrong happened. For all these reasons the experiment was repeated more carefully in order to decide which were the best conditions to use in further experiments.

All the after experiments did not work properly and the identification any of the targets in any of the samples were not possible. Therefore, after many different unsuccessful attempts and experimental designs, the RNA integrity of the samples was mandatory to assess to detect the experimental problem. Moreover, for this purpose a non-denaturing RNA agarose gel was performed to assess the quality of the RNA samples, being chosen one or two control samples from each experiment done until then to assess. The results are shown below in **Figure 4.10**.

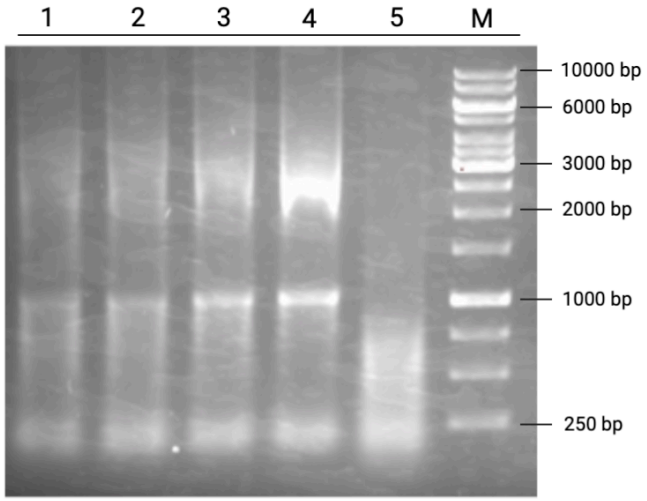

Figure 4.10 - Representation of the RNA samples in an 1% non-denaturating RNA agarose gel. Lanes 1 and 2 are two control samples from the first experiment; Lanes 3 and 4 are control samples from the experiment 2; lane 5 is a control sample from the last experiment; and lane M is the O'GeneRuler 1kb DNA Ladder.

In **Figure 4.10**, the sample in lane 5 is degraded, but all the other ones are good, since they show three bands in the gel, corresponding to small RNAs and the two subunits of the RNA molecule, 18S and 28S (from the bottom to the top of the gel). From these results, since the last experiment seemed to have its samples degraded, an RNA extraction from the two used cell lines with the number of cells recommended by the manufacturer's protocol was repeated. Below are the obtained results for this experiment, **Figure 4.11**.

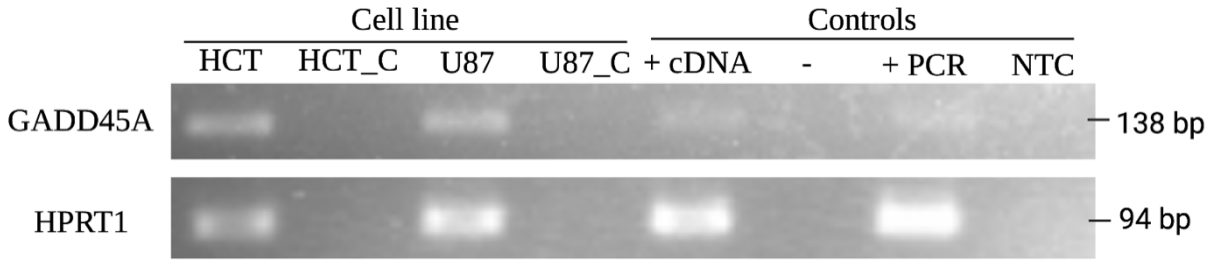

Figure 4.11 - Representation of the new PCR samples for GADD45A and HPRT1 targets in a 2% agarose gel. Lane 'HCT' is the sample with material extracted from the HCT-116 cell line; lane 'HCT_C' is the same sample of the lane before but with no RT; lane 'U87' is the sample with material extracted from U87MG cell line; lane 'U87_C' is the same sample of the lane before but without RT ; lane '+ cDNA' - positive PCR product control from a RNA sample control, lane '-' - PCR product from a RNA sample control without reverse transcriptase, lane '+PCR' – positive PCR product from a cDNA sample control, lane 'NTC' - non-template control.

The results showed in **Figure 4.11**, lead to the conclusion that the RNA extraction, the cDNA synthesis, and the PCR protocols were working properly, since the gel contain bands in the each well loaded with PCR product sample and the control wells are empty. As the next step, since the protocols were working properly, the first experiment was repeated as desired, and the results are represented above (**Figure 4.12**).

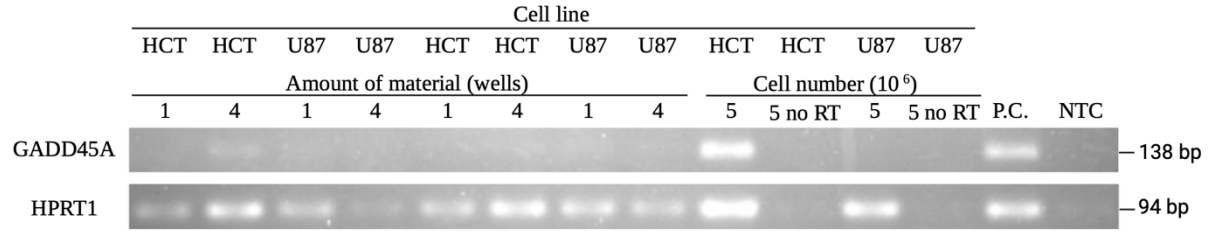

Figure 4.12 - Representation of the PCR products of GADD45A and HPRT1 genes in a 2% agarose gel. HCT – HCT-116 cell line; U87 – U87MG cell line; PC – positive control sample, NTC - non-template control.

By the results represented in **Figure 4.12**, we can conclude that material from one well is enough to detect a housekeeping gene, like HPRT1, but not for a low expression gene like GADD45A. Therefore, the amount of biological material decided that should be used for the next experiments using the qRT-PCR technique is from four wells. Moreover, with the protocol for detecting differences gene expression for both cell culture models being established was possible to move on to the chemotherapeutic drugs experiments.

4.2. Cell viability seems to be culture model and cell line dependent upon chemotherapeutic drug treatment.

As mentioned previously, some studies show evidence that the 3D spheroid cell culture method can be more similar to the solid tumours when compared to the traditional 2D cell culture model. Furthermore, although some of them shown that the cell viability and cell death upon treatment with commonly used chemotherapeutic drugs is cell culture method dependent in colorectal cancer and glioblastoma cell lines, it is still needed further analysis (Karlsson et al., 2012; Lv et al., 2016). Therefore, to assess and compare the cell viability of the HCT-116 and U87 MG cell lines upon treatment with 500μM of 5-FU and TMZ, respectively, an MTS assay was performed (**Figure 4.13**). The chosen drugs concentration was decided having in consideration the Greenman lab work experience and evidence in the literature of an effect in cell viability by this concentration of drug in the used cell lines (Kanzawa et al., 2003; Tawfik et al., 2017).

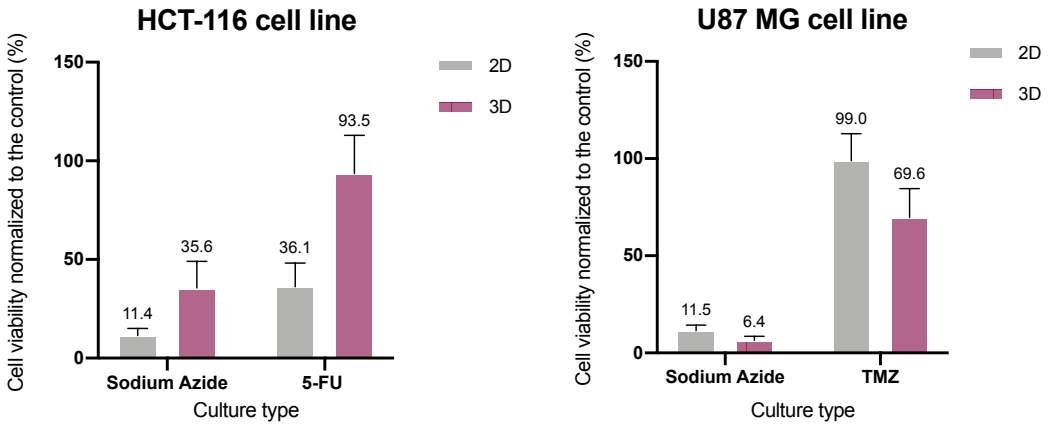

Figure 4.13 - Comparison of the percentages mean normalized to the control group of the cell viability of both cell lines treated in 2D and 3D cell culture models. It was performed the mean of the four independent biological replicates. S.A – treatment with sodium azide, as positive control of the assay; S.A. – HCT-116 – treatment with sodium azide in the HCT-116 cell line; S.A. – U87 – treatment with sodium azide in the U87-MG cell line; 5-FU – treatment with 5-FU in the HCT-117 cell line; TMZ – treatment with TMZ in the U87-MG cell line. The error bars were calculated using the SEM of the biological triplicates. P-values were assessed by a statistical paired t test and indicated as followed: P<0,033 (*), P<0,002 (**), P<0,0002 (***) and P<0,0001 (****).

Since the mean of the cell viability results from the four experiments for the U87 MG cell line did not show a statistical difference between cell culture models, the results of the four independent experiments are represented in **Supplementary Figure 7.1**. Although the results are not statistically significant, the HCT-116 cells cultured in 2D upon treatment with 5-FU seems to show a lower cell viability percentage when compared to the cells cultured in 3D (**Figure 4.13**). The U87 MG cell line show different results when compared to the HCT-116 cell line. For the U87 MG cell line, the differences between the 2D cultured cells and the 3D ones show a higher variability between the four experiments (**Supplementary Figure 7.1**). As shown in **Figure 4.13**, the 2D U87 MG cells seems to show a higher cell viability upon TMZ treatment when compared to the 3D ones. The treatment with sodium azide was used as a positive control of the assay in order to make sure that the assay was actually working by detecting a lower cell viability in treated cells. Since the cell number was optimized for each cell line prior to the chemotherapeutic drugs experiments, having in consideration the proliferation rate of each cell and the MTS assay optimization results, the number of seeded cells for each cell line was different. Therefore, as the results show, the two cell lines show a different behavior from each other upon 2D and 3D cell culture models with drug treatment, which can be related to biological mechanisms influenced by the seeding cell number. In addition, we can conclude that, for the HCT-116 cell line, the cell viability of 5-FU treated cells seems to be dependent of the cell culture model, but for the U87 MG cell line, it is not possible to conclude that the cell culture model influences the cell viability upon TMZ treatment.

4.3. Cell cycle and cell proliferation genes expression seems to be influenced by the cell culture model.

To further analyse the impact of the cell culture model in the cell's behaviour upon chemotherapeutic drug treatment, the expression of cell cycle arrest and proliferation genes was assessed in treated and control samples. The RNA was extracted from the four control and four treated cells from both cell lines, the cDNA synthesized, and the qPCR performed for GADD45A, CDKN1A and cMyc genes, using HPRT1 as internal control (**Figure 4.14**). Since the mean of the four experiments results (**Supplementary Figure 7.2**Erro! A origem da referência não foi encontrada.) showed a high variability

between the four biological independent experiments, the results were presented as individual experiments in order to discuss them in more depth.

The gene expression of GADD45A in the treated HCT-116 cells with 5-FU seems to show a difference between the cells cultured in 2D and 3D (**Figure 4.14B** and **D**). Except for the experiment 1, the gene expression of GADD45A in HCT-116 cells cultured in 3D upon treatment is higher when compared to the ones cultured in 2D, upon 5-FU treatment (**Figure 4.14B, C** and **D**). The expression of GADD45A gene is up-regulated upon 5-FU treatment in HCT-116 cells, despite the cell culture model used, excluding the experiment 4 (**Figure 4.14A, B** and **C**). However, the 3D method seams to enhance the expression of this gene even more compared to the 2D upon chemotherapeutic treatment. In the TMZ treated U87 MG cell line, although the difference between the 2D and 3D GADD45A gene expression looks it is not significant, the results show a tendency of up-regulation of GADD45A in cells cultured in 2D model than in cells using the 3D one (**Figure 4.14**). Therefore, appears to show an opposite behaviour compared to 5-FU treated HCT-116 cell line. However, both cell lines show an up-regulation in GADD45A gene expression upon treatment when compared to the control.

The CDKN1A gene expression shows very inconsistence results between biological replicates for the HCT-116 cell line upon treatment (**Figure 4.14**). However, it is possible to observe an up-regulation of the CDKN1A upon 5-FU treatment in both cell culture models. Therefore, it is not possible to conclude that this gene is expressed differently in cells cultured in 2D and 3D, and further assessment was needed. For the U87 MG cell line the results show an up-regulation of CDKN1A gene in cells both cultured in 2D and 3D, upon TMZ treatment (**Figure 4.14**). Furthermore, although not all experiments show this result, it appears that the up-regulation of this gene is higher in the 2D than in the 3D method (**Figure 4.14B** and **C**).

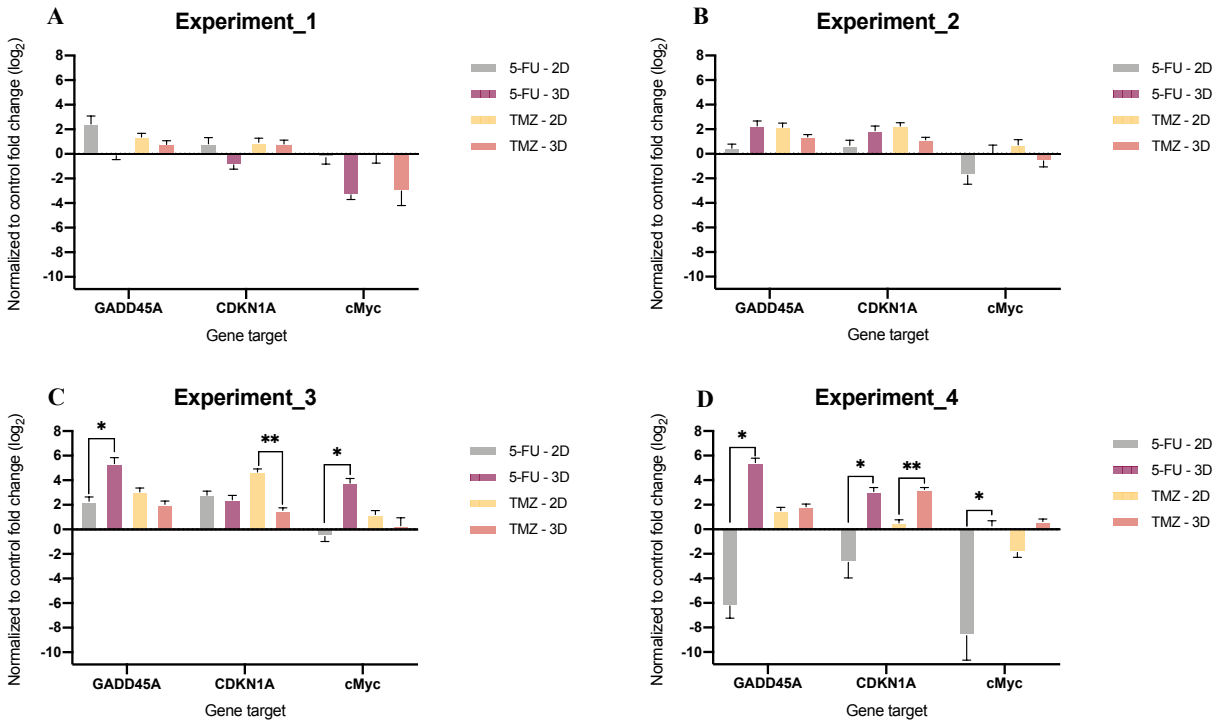

Figure 4.14 - Comparison of the GADD45A, CDKN1A and c-Myc genes fold change of both cell lines treated samples in 2D and 3D culture methods. It was performed four independent experiments as biological replicates, but since the results were not consistent between experiments it was decided to present them individually instead of in the mean form. 5-FU – treatment with 5-FU in the HCT-117 cell line; TMZ – treatment with TMZ in the U87-MG cell line. The error bars were calculated from the SEM of the technical triplicates and with error propagation. P-values were assessed by a statistical t test and indicated as followed: P<0,033 (*), P<0,002 (**) and P<0,001 (***).

In 5-FU treated HCT-116 cell line, the gene expression of c-Myc is down-regulated in cells cultured with the 2D method compared to the control (**Figure 4.14**). However, the treated cells cultured in 3D show a different behaviour, since the c-Myc expression show no difference between the treated and control cells, excepting the experiments 1 and 3 where it shows opposite results (**Figure 4.14B** and **D**). Furthermore, it seems that the culture method used upon chemotherapeutic drug treatment influence the c-Myc gene expression. The TMZ treated U87 MG cells show a different result from the HCT-116, since there is no significant difference between the c-Myc expression in the 2D cells and the 3D ones (**Figure 4.14**). Furthermore, due to the opposite results obtained in each experiment, it is not possible to conclude whether the TMZ treatment in U87 MG causes the change in c-Myc gene expression.

4.4. Cells follow a 3D layered spatial distribution within the spheroids.

As previously described in the literature, usually the cells have a specific distribution within the spheroids, with proliferative cells present in the external layer and apoptotic and senescent cells located deeper in the 3D structure. In order to assess if our cultured spheroids presented this type of structural arrangement and how the chemotherapeutic drug treatment influenced it, we performed immunohistochemistry assays using the proliferation marker Ki-67, Rhodamine-Phalloiding staining for actin, and DAPI staining to identify cell nuclei. Furthermore, since the previous results from cell viability and gene expression have shown big variability within the biological replicates, it was also important to assess the spheroid integrity (**Figure 4.15**).

We observed that the HCT-116 spheroids presented, a well-defined external layer of proliferating cells, typical of these 3D structures, since the cells marked with the Ki-67 marker were mainly present in the outer layer of the spheroid (**Figure 4.15**). Furthermore, upon 5-FU treatment, the spheroids were much smaller than the control and the distribution the few proliferating cells no longer accumulated at the external layer of the spheroid (**Figure 4.15**). Therefore, it is possible to conclude that the chemotherapeutic drug had an effect in the spheroid, since the number of proliferative cells decreased, the 3D structure was affected, and the spheroid size decreased too. The U87 MG spheroids show a much less evident outer layer of proliferating cells, but they still show less Ki-67 marked cells in the spheroid core (**Figure 4.15**). Interestingly, upon the TMZ treatment, it was not possible to observe any evidence of changes in the 3D structure of the U87 MG spheroids, showing that this cell line could overcome the chemotherapeutic drug effects (**Figure 4.15**). This observation was confirmed by parallel results obtained in 2D cultures (**Table 4.1**). The treatment with the chemotherapeutic drug for both cell lines had an impact in cell proliferation since the Ki-67 positives decrease upon treatment. Furthermore, it was also possible to observe a higher difference between the control and the treated cells for the HCT-116 cell line in comparison to the U87 MG (**Table 4.1**). However, this technique showed a few technical problems, since the control wells had a high cell confluence and, therefore, during the immunofluorescence protocol part of the cells detached from the well bottom. Furthermore, the results showed are only form one experiment due to protocol adaptations and time restrictions. Therefore, this technique did not show technical reproducibility and further experiments will be needed to reach an accurate conclusion about these results.

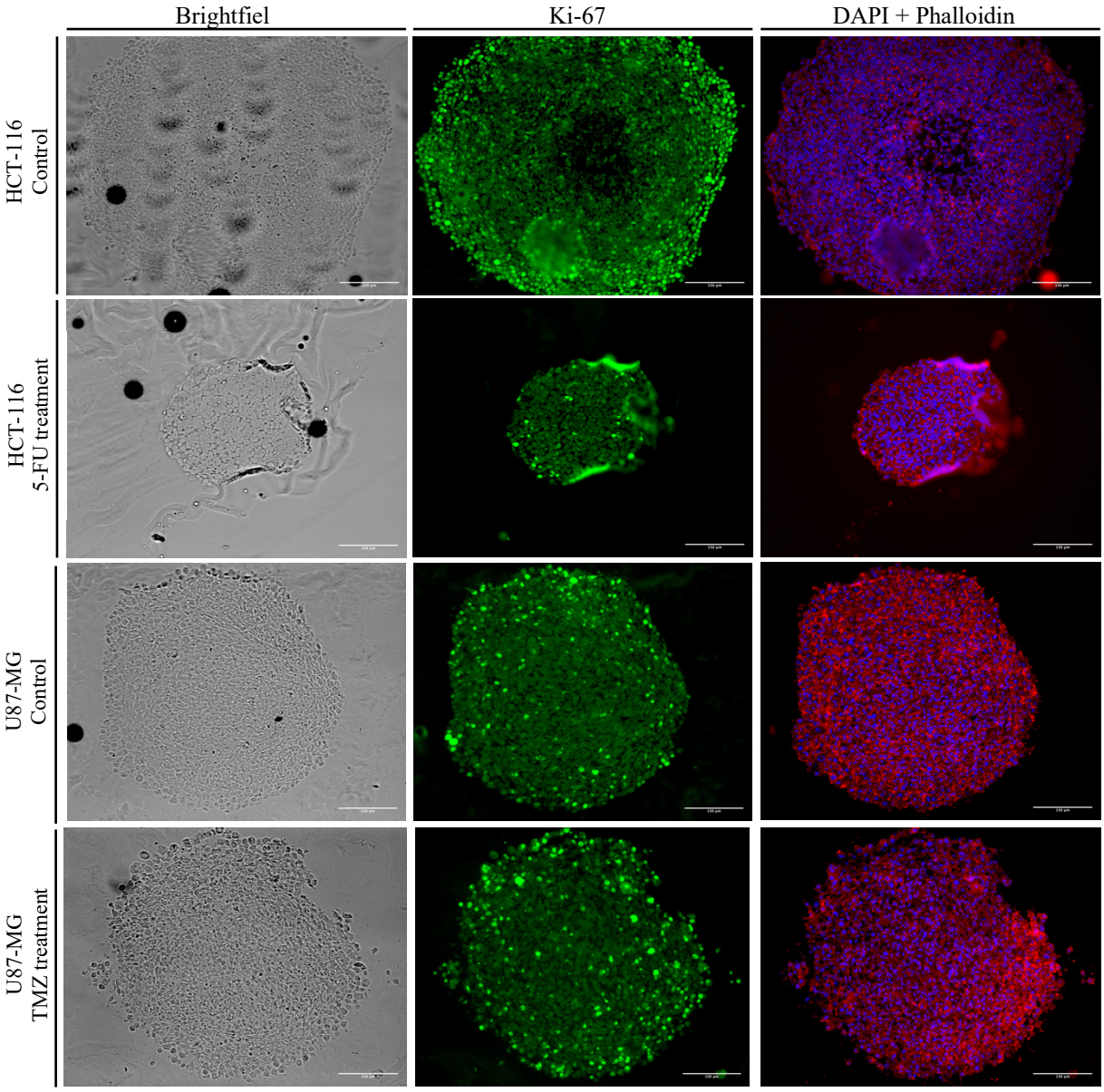

Figure 4.15 - Cell proliferation within the spheroid upon chemotherapeutic drug treatment by immunohistochemistry. The Ki-67 antibody was used to assess the cells in proliferation. DAPI and phalloidin – DAPI staining of the nucleus and rhodamine phalloidin to stain the cell's membrane. Images obtained with an ampliation of 10x and analysed in Fiji.

Table 4.1 – Immunofluorescent results in 2D cell culture model upon chemotherapeutic drug treatment. The cells were identified using the rhodamine-phalloidin staining and the total and the positive cells counted using the CellProfiler software. NEG - cells which intensity of Ki-67 marker were lower than 15.000; POS - cells which intensity of Ki-67 marker were higher than 15.000. % POS – percentage of positive cells. The p-value was calculated using the chi-square test using the GraphPad software.

HCT-116 cell line					
	NEG	POS	Total	% POS	p-value
5-FU	78	2	80	2,50	<0,0001 (****)
Control	247	235	482	48,80	
U87 MG cell line					
	NEG	POS	Total	% POS	p-value
TMZ	788	9	797	1,13	<0,0001 (****)
Control	73	9	82	11,00	

In summary, the immunofluorescence approach allowed us to conclude that the spheroids were formed properly in our culture conditions and that the results variability was unlikely to be caused by the integrity of the spheroids. Furthermore, they highlight differences in the behaviour of the two cell lines and their response to the chemotherapeutic agents used in this work.

5. Discussion

The usage of 2D cell culture models had an extreme importance in the past to reach the knowledge that we have today, however, it is well known that this type of models does not reflect how tumours behave in vivo. Therefore, it is important to study the tumour's characteristics using different models, such as 3D and microfluidic devices in order to develop better models for drug screening. Within this topic, this work aims for the comparison of three cell cultured methods by assessing cell viability, gene expression, spheroid spatial organization and cell proliferation, upon chemotherapeutic drug treatment.

As described in the literature, the 3D structure of the spheroid is responsible for the lower efficacy of the drugs when compared to the usual 2D model. The layered structure of the spheroids leads to the presence of cells that can be found in three main stages of the cell cycle: proliferation, senescence and necrotic. Therefore, chemotherapeutic drugs that affect the cell cycle and need the cells to be in a proliferative state, such as 5-FU and TMZ, will not be effective in every cell that composes the spheroid (Costa et al., 2016). For these reasons, upon treatment with commonly used drugs, was expected that the spheroids would have shown higher cell viability when compared to the cells cultured in 2D. As a cell viability measure, the MTS assay was used and the HCT-116 cell line showed the expected behaviour, with the spheroids showing higher cell viability than the 2D cells, upon 5-FU treatment. However, for the U87 MG cell line, there was no difference in cell viability between the two cell cultures upon TMZ treatment. Before the execution of the experiment using the chemotherapeutic drugs, the MTS assay was optimized for the best cell seeding conditions and incubation time with the reagent. This optimization led to the seeding of different cell number for each cell line and culture type, since the HCT-116 cell line has a two to three times faster growth than the U87 MG cell line, which could influence the cellular responses to the chemotherapeutic drugs. Although the origin of U87-MG cell line has been questioned, its human glioblastoma origin was confirmed (Allen et al., 2016, p. 87). Therefore, this type of cancer is well known for being one of the cancers with higher heterogeneity. A small difference in proliferation or death rate between tumour clones can lead to the predominance of one of them within the tumour population. Furthermore, Davis et al., showed that drug resistance can be a direct result of this type of clonal cooperation even if no individual clone is drug resistant (Davis et al., 2019). Furthermore, they showed that clones can dynamically adjusted their growth rates positively and negatively, independent of released factors, which might mean that heterogeneity is an intrinsic property of cancer cells. Therefore, a possible reason for the cell viability being similar to the cells grown under the two different cell culture models upon treatment could be the presence of high heterogeneity. Since U87 MG is a highly heterogeneous cell line makes it possible to have the mechanisms to select the survival clones within the cells upon the TMZ treatment, causing an increase in drug resistance in the 2D model, although the three-dimensional structure is absent.

The GADD45A gene is known to be involved in DNA repair, genomic stability, and cell cycle arrest at G2/M check point as a response to stress, and its defective expression leads to increased tumorigenesis (Liu et al., 2018; H.-H. Wang et al., 2017). This gene also plays an important role in inhibition of angiogenesis, where it acts as a tumour suppressor by the blockage of the mTOR/STAT3 pathway. However, the presence of abnormal expression of GADD45A has been found in different types of solid tumours, therefore, revealing that this gene might improve tumour survival (Salvador et al., 2013). Several studies showed that GADD45A induction was associated with lower patient survival rate in pancreatic samples and a protection of melanoma cells from UV radiation-induced deaths, and that the lack of this gene is correlated to a good response to radiotherapy in cervical carcinomas (Liu et al., 2018, p.; Salvador et al., 2013). In glioblastoma, GADD45A was found to play a protective role against TMZ treatment through TP53-dependent and MGMT-dependent pathway in U87 MG cells, and the knock-down of this gene leads to more sensible cells to the treatment (H.-H. Wang et al., 2017). In a study using HCT-116 cell line and 2 resistant cell lines derived from this one, they showed that GADD45A

was up-regulated in all cell lines upon 5-FU treatment, but with higher expression in one of the resistant cell lines (P. M. De Angelis et al., 2006). From the results obtained in this present study, in the HCT-116 cell line, the GADD45A gene expression was up-regulated upon treatment with 5-FU, and with higher up-regulation in the 3D cell culture model. Furthermore, the results from the cell viability assay showed that the 3D culture method presented a higher viability upon 5-FU treatment when compared to the 2D one. Therefore, it is possible to conclude that the cell viability of this cell line upon treatment maybe GADD45A dependent, and that this gene may play a protective role in colorectal cancer cell line upon 5-FU treatment. In the U87 MG cell line, the cell viability assay showed almost no difference between the two cell culture models, however, the 2D model seems to have shown a tendency to have higher viability upon TMZ treatment. In addition, when the GADD45A expression is investigated in this cell line, it is possible to observe almost no difference between the cell culture models, but with a tendency of higher expression of this gene in the 2D model, upon treatment. Therefore, it is possible to conclude that in this cell line, the unexpected higher cell viability in the 2D model, upon TMZ treatment, in comparison to the 3D one, maybe due to the higher expression of GADD45A in 2D.

The CDKN1A, which is a CDK regulator and a cell cycle G1/S phase suppressor, is involved in inhibiting the cellular proliferation and promotes senescence, and usually acts as a tumour suppressor implicated in many cancer treatments. Therefore, the induction of CDKN1A could be a way to prevent tumour growth and metastasis (Ye et al., 2021). However, recent studies showed that under certain conditions, this gene can promote cellular proliferation and act as an oncogene. In line with its dual role, its overexpression in gliomas is found to be linked to its oncogenic activity, but in colorectal cancer its down-regulation is linked to poor diagnosis. Upon chemotherapeutic drug treatment studies show for both glioblastoma and colorectal cancer an up-regulation of the CDKN1A gene (P. M. De Angelis et al., 2006; Ye et al., 2021). From the results of this study is possible to observe a similar behaviour of GADD45A and CDKN1A expression upon treatment. Since both these genes are transcriptional targets of p53 (Ramos et al., 2021), which is a tumour-suppressor involved in cellular response to DNA damaging agents, it was expected that both were up-regulated. Furthermore, as some studies in colorectal cancer and glioblastoma show, this gene seems to be involved in resistance mechanisms to the treatment, as GADD45A (P. M. De Angelis et al., 2006; Hu et al., 2021).

The protooncogene c-Myc plays a central role in regulating cell growth and differentiation and, thus the cellular proliferation, migration and angiogenesis. Although the c-Myc is present in higher levels in approximately 70% of the human colon tumours, it is not necessarily a negative prognostic factor since it has been associated with the increase in cell sensitivity to apoptosis (Abaza et al., 2008; L. Wang et al., 2016). Hypoxia factors (HIFs), which are crucial for cellular responses mediation to hypoxia, regulate the c-Myc oncogene, being downregulated in specific regions of solid tumours that the presence of oxygen is low. Therefore, the down-regulation of c-Myc leads to cell cycle arrest and, consequently resistance to chemotherapeutic agents that rely on DNA replication, such as 5-FU and TMZ (L. Wang et al., 2016). In this study, the results for c-Myc gene expression for both cell lines present big variability, therefore being very difficult to assess the impact of drug treatment in the cell lines and the impact of the used cell culture models. In the HCT-116 cell line, the 2D cell culture model shows lower cell viability upon 5-FU treatment and down-regulation of c-Myc. Therefore, this can lead to the conclusion that maybe the c-Myc is acting as a proliferation promoter and consequently leading to an increase of effectiveness of the 5-FU in the cells, due to their DNA replication. The HCT-116 cell line grown under 3D conditions show no difference overall in c-Myc expression in comparison to the control. This observation can possibly be explained by the presence of a big fraction of the cells within the spheroid located in a low-oxygen layer in which the c-Myc is down-regulated, leading to 5-FU resistance, which is also supported by the higher cell viability. In the U87 MG cell line the results of c-Myc gene expression, upon treatment, also has a lot of variability, therefore it will be needed more gene expression analysis in order to get to a conclusion.

The 3D spheroids are cellular aggregates that better mimic the physical communications and signalling pathways of solid tumours. Its internal structure is composed of three main layers of cells in different stages of the cell cycle, being the outside one where the cells are in a proliferative stage and the core where cells are in necrotic stage. This type of 3D structure leads to the chemotherapeutic drugs having different effects in the cells depending on their location and cell cycle stage (Costa et al., 2016). In this present study it was possible to demonstrate, by immunohistochemistry, that the produced spheroids formed this type of 3D structure. The HCT-116 spheroids had a very evident outer layer of proliferating cells, marked with the proliferation marker Ki-67, therefore, in agreement with the cell viability results and gene expression, where the 3D cell culture models had higher resistance to 5-FU treatment than 2D cells. The U87 MG showed a less evident outer layer of cells in proliferation and a lower impact of the TMZ treatment in the 3D structure of the spheroids. However, this agrees with the tumour heterogeneity described in the literature that can be a possible reason for the different behaviour in cell viability and gene expression and, therefore in 3D structure. The analysis by immunofluorescence of the 2D cell culture model upon treatment matches the 3D immunohistochemistry results previously shown. The chemotherapeutic drugs had an effect in both cell lines, however the U87 MG showed a much less evident difference between the control and the treated cells. This result means that the TMZ has an impact in the number of proliferating cells in 2D but similar to the control, which agrees with the previous cell viability results.

The results obtained in this work show a big variability between biological replicates for both cell lines and cell culture methods. Although both quantitative methods, MTS and qRT-PCR, show high variability, the qRT-PCR is the one with higher deviation. Therefore, since the experimental process from the RNA extraction until the qRT-PCR were done separately from each biological replicate, it is a possibility that this could explain a higher variability between experiments. In addition, the small and different amounts of RNA extracted from the samples of each biological replicate and, therefore, used as template for the qRT-PCR reactions, could also contribute for the increase in variability. Furthermore, it was also possible to detect that the TMZ seemed to not be working properly, since it showed almost no impact in the U87 MG cell line. Therefore, although the used drug was similar to the one used in the Greenman Lab it seems to not be working in the same way, being a possibility that the biological behaviour of the drug within the cell could be slightly different. In agreement, for further analysis it should be done a dose-response curve to detect the best drug concentration for each cell line and treatment in order to have more conclusive results in the comparison of the cell culture methods.

In conclusion, this work is a contribution for the assessment of the main differences in cellular viability, gene expression, proliferation, and spatial organization of the cells within two cell culture models upon chemotherapeutic drug treatment. Moreover, further experiments to confirm some of the results obtained will be needed, since the variability of them was high. However, the results presented here agree that cellular response is influenced by the *in vitro* models used, thus the improvement of new models increasingly similar to human tumours is of extreme importance.

6. Bibliography

Abaza, M.-S. I., Al-Saffar, A., Al-Sawan, S., & Al-Attiyah, R. (2008). C-*myc* Antisense Oligonucleotides Sensitize Human Colorectal Cancer Cells to Chemotherapeutic Drugs. *Tumor Biology*, *29*(5), 287–303. https://doi.org/10.1159/000156706

Allen, M., Bjerke, M., Edlund, H., Nelander, S., & Westermark, B. (2016). Origin of the U87MG glioma cell line: Good news and bad news. *Science Translational Medicine*, *8*(354), 354re3-354re3. https://doi.org/10.1126/scitranslmed.aaf6853

Antoni, D., Burckel, H., Josset, E., & Noel, G. (2015). Three-Dimensional Cell Culture: A Breakthrough in Vivo. *International Journal of Molecular Sciences*, *16*(12), 5517–5527. https://doi.org/10.3390/ijms16035517

Arvelo, F. (2015). Biology of colorectal cancer. *Ecancermedicalscience*, *9*. https://doi.org/10.3332/ecancer.2015.520

Baghban, R., Roshangar, L., Jahanban-Esfahlan, R., Seidi, K., Ebrahimi-Kalan, A., Jaymand, M., Kolahian, S., Javaheri, T., & Zare, P. (2020). Tumor microenvironment complexity and therapeutic implications at a glance. *Cell Communication and Signaling*, *18*(1), 59. https://doi.org/10.1186/s12964-020-0530-4

Blondy, S., David, V., Verdier, M., Mathonnet, M., Perraud, A., & Christou, N. (2020). 5-Fluorouracil resistance mechanisms in colorectal cancer: From classical pathways to promising processes. *Cancer Science*, *111*(9), 3142–3154. https://doi.org/10.1111/cas.14532

Breslin, S., & O'Driscoll, L. (2013). Three-dimensional cell culture: The missing link in drug discovery. *Drug Discovery Today*, *18*(5–6), 240–249. https://doi.org/10.1016/j.drudis.2012.10.003

Chen, H., Cheng, Y., Wang, X., Wang, J., Shi, X., Li, X., Tan, W., & Tan, Z. (2020). 3D printed *in vitro* tumor tissue model of colorectal cancer. *Theranostics*, *10*(26), 12127–12143. https://doi.org/10.7150/thno.52450

Costa, E. C., Moreira, A. F., de Melo-Diogo, D., Gaspar, V. M., Carvalho, M. P., & Correia, I. J. (2016). 3D tumor spheroids: An overview on the tools and techniques used for their analysis. *Biotechnology Advances*, *34*(8), 1427–1441. https://doi.org/10.1016/j.biotechadv.2016.11.002

Courau, T., Bonnereau, J., Chicoteau, J., Bottois, H., Remark, R., Assante Miranda, L., Toubert, A., Blery, M., Aparicio, T., Allez, M., & Le Bourhis, L. (2019). Cocultures of human colorectal tumor spheroids with immune cells reveal the therapeutic potential of MICA/B and NKG2A targeting for cancer treatment. *Journal for ImmunoTherapy of Cancer*, *7*(1), 74. https://doi.org/10.1186/s40425-019-0553-9

Damiati, S., Kompella, U., Damiati, S., & Kodzius, R. (2018). Microfluidic Devices for Drug Delivery Systems and Drug Screening. *Genes*, *9*(2), 103. https://doi.org/10.3390/genes9020103

Davis, J. B., Krishna, S. S., Jomaa, R. A., Duong, C. T., Espina, V., Liotta, L. A., & Mueller, C. (2019). *OPEN A new model isolates glioblastoma clonal interactions and reveals unexpected modes for regulating motility, proliferation, and drug resistance*. 14.

Dawson, A., Green, V., Bower, R., & Greenman, J. (2016). *Microfluidics: The fur-free way towards personalised medicine in cancer therapy*. 6.

De Angelis, P., Fjell, B., Kravik, K., Haug, T., Tunheim, S., Reichelt, W., Beigi, M., Clausen, O., Galteland, E., & Stokke, T. (2004). Molecular characterizations of derivatives of HCT116 colorectal cancer cells that are resistant to the chemotherapeutic agent 5-fluorouracil. *International Journal of Oncology*. https://doi.org/10.3892/ijo.24.5.1279

De Angelis, P. M., Svendsrud, D. H., Kravik, K. L., & Stokke, T. (2006). Cellular response to 5-fluorouracil (5-FU) in 5-FU-resistant colon cancer cell lines during treatment and recovery. *Molecular Cancer*, *5*(1), 20. https://doi.org/10.1186/1476-4598-5-20

Devarasetty, M., Dominijanni, A., Herberg, S., Shelkey, E., Skardal, A., & Soker, S. (2020).

Simulating the human colorectal cancer microenvironment in 3D tumor-stroma co-cultures in vitro and in vivo. *Scientific Reports*, *10*(1), 9832. https://doi.org/10.1038/s41598-020-66785-1

Drost, J., & Clevers, H. (2018). Organoids in cancer research. *Nature Reviews Cancer*, *18*(7), 407–418. https://doi.org/10.1038/s41568-018-0007-6

Giraldo, N. A., Sanchez-Salas, R., Peske, J. D., Vano, Y., Becht, E., Petitprez, F., Validire, P., Ingels, A., Cathelineau, X., Fridman, W. H., & Sautès-Fridman, C. (2019). The clinical role of the TME in solid cancer. *British Journal of Cancer*, *120*(1), 45–53. https://doi.org/10.1038/s41416-018-0327-z

Gunti, S., Hoke, A. T. K., Vu, K. P., & London, N. R. (2021). Organoid and Spheroid Tumor Models: Techniques and Applications. *Cancers*, *13*(4), 874. https://doi.org/10.3390/cancers13040874

Hanahan, D., & Weinberg, R. A. (2000). The Hallmarks of Cancer. *Cell*, *100*(1), 57–70. https://doi.org/10.1016/S0092-8674(00)81683-9

Harrington, K. J. (2016). The biology of cancer. *Medicine*, *44*(1), 1–5. https://doi.org/10.1016/j.mpmed.2015.10.005

Hu, K., Li, J., Wu, G., Zhou, L., Wang, X., Yan, Y., & Xu, Z. (2021). The novel roles of virus infection-associated gene CDKN1A in chemoresistance and immune infiltration of glioblastoma. *Aging*, *13*(5), 6662–6680. https://doi.org/10.18632/aging.202519

Jensen, C., & Teng, Y. (2020). Is It Time to Start Transitioning From 2D to 3D Cell Culture? *Frontiers in Molecular Biosciences*, *7*, 33. https://doi.org/10.3389/fmolb.2020.00033

Kahlert, U. D., Mooney, S. M., Natsumeda, M., Steiger, H.-J., & Maciaczyk, J. (2017). Targeting cancer stem-like cells in glioblastoma and colorectal cancer through metabolic pathways: Metabolism of cancer stem-like cells. *International Journal of Cancer*, *140*(1), 10–22. https://doi.org/10.1002/ijc.30259

Kanzawa, T., Germano, I. M., Kondo, Y., Ito, H., Kyo, S., & Kondo, S. (2003). Inhibition of telomerase activity in malignant glioma cells correlates with their sensitivity to temozolomide. *British Journal of Cancer*, *89*(5), 922–929. https://doi.org/10.1038/sj.bjc.6601193

Karlsson, H., Fryknäs, M., Larsson, R., & Nygren, P. (2012). Loss of cancer drug activity in colon cancer HCT-116 cells during spheroid formation in a new 3-D spheroid cell culture system. *Experimental Cell Research*, *318*(13), 1577–1585. https://doi.org/10.1016/j.yexcr.2012.03.026

Kesari, S. (2011). Understanding Glioblastoma Tumor Biology: The Potential to Improve Current Diagnosis and Treatments. *Seminars in Oncology*, *38*, S2–S10. https://doi.org/10.1053/j.seminoncol.2011.09.005

Lee, S.-H., Hong, J. H., Park, H. K., Park, J. S., Kim, B.-K., Lee, J.-Y., Jeong, J. Y., Yoon, G. S., Inoue, M., Choi, G.-S., & Lee, I.-K. (2015). Colorectal cancer-derived tumor spheroids retain the characteristics of original tumors. *Cancer Letters*, *367*(1), 34–42. https://doi.org/10.1016/j.canlet.2015.06.024

Li, Z., & Cui, Z. (2014). Three-dimensional perfused cell culture. *Biotechnology Advances*, *32*(2), 243–254. https://doi.org/10.1016/j.biotechadv.2013.10.006

Liu, J., Jiang, G., Mao, P., Zhang, J., Zhang, L., Liu, L., Wang, J., Owusu, L., Ren, B., Tang, Y., & Li, W. (2018). Down-regulation of GADD45A enhances chemosensitivity in melanoma. *Scientific Reports*, *8*(1), 4111. https://doi.org/10.1038/s41598-018-22484-6

Longley, D. B., Harkin, D. P., & Johnston, P. G. (2003). 5-Fluorouracil: Mechanisms of action and clinical strategies. *Nature Reviews Cancer*, *3*(5), 330–338. https://doi.org/10.1038/nrc1074

Luca, A. C., Mersch, S., Deenen, R., Schmidt, S., Messner, I., Schäfer, K.-L., Baldus, S. E., Huckenbeck, W., Piekorz, R. P., Knoefel, W. T., Krieg, A., & Stoecklein, N. H. (2013). Impact of the 3D Microenvironment on Phenotype, Gene Expression, and EGFR Inhibition of Colorectal Cancer Cell Lines. *PLoS ONE*, *8*(3), e59689. https://doi.org/10.1371/journal.pone.0059689

Lv, D., Yu, S., Ping, Y., Wu, H., Zhao, X., Zhang, H., Cui, Y., Chen, B., Zhang, X., Dai, J., Bian, X., & Yao, X. (2016). A three-dimensional collagen scaffold cell culture system for screening anti-

glioma therapeutics. *Oncotarget*, *7*(35), 56904–56914. https://doi.org/10.18632/oncotarget.10885

Maira, M.-S., Pearson, M. A., Fabbro, D., & García-Echeverría, C. (2007). Cancer Biology. In *Comprehensive Medicinal Chemistry II* (pp. 1–31). Elsevier. https://doi.org/10.1016/B0-08-045044-X/00202-9

Mármol, I., Sánchez-de-Diego, C., Pradilla Dieste, A., Cerrada, E., & Rodriguez Yoldi, M. (2017). Colorectal Carcinoma: A General Overview and Future Perspectives in Colorectal Cancer. *International Journal of Molecular Sciences*, *18*(1), 197. https://doi.org/10.3390/ijms18010197

Messerschmidt, J. L., Prendergast, G. C., & Messerschmidt, G. L. (2016). How Cancers Escape Immune Destruction and Mechanisms of Action for the New Significantly Active Immune Therapies: Helping Nonimmunologists Decipher Recent Advances. *The Oncologist*, *21*(2), 233–243. https://doi.org/10.1634/theoncologist.2015-0282

Musah-Eroje, A., & Watson, S. (2019). A novel 3D in vitro model of glioblastoma reveals resistance to temozolomide which was potentiated by hypoxia. *Journal of Neuro-Oncology*, *142*(2), 231–240. https://doi.org/10.1007/s11060-019-03107-0

Neufeld, L., Yeini, E., Reisman, N., Shtilerman, Y., Ben-Shushan, D., Pozzi, S., Madi, A., Tiram, G., Eldar-Boock, A., Ferber, S., Grossman, R., Ram, Z., & Satchi-Fainaro, R. (2021). Microengineered perfusable 3D-bioprinted glioblastoma model for in vivo mimicry of tumor microenvironment. *Science Advances*, *7*(34), eabi9119. https://doi.org/10.1126/sciadv.abi9119

Nunes, A. S., Barros, A. S., Costa, E. C., Moreira, A. F., & Correia, I. J. (2019). 3D tumor spheroids as in vitro models to mimic in vivo human solid tumors resistance to therapeutic drugs: NUNES ET AL. *Biotechnology and Bioengineering*, *116*(1), 206–226. https://doi.org/10.1002/bit.26845

Olubajo, F., Achawal, S., & Greenman, J. (2020). Development of a Microfluidic Culture Paradigm for Ex Vivo Maintenance of Human Glioblastoma Tissue: A New Glioblastoma Model? *Translational Oncology*, *13*(1), 1–10. https://doi.org/10.1016/j.tranon.2019.09.002

Passardi, A., Scarpi, E., & Ulivi, P. (2020). Molecular and Translational Research on Colorectal Cancer. *International Journal of Molecular Sciences*, *21*(11), 4105. https://doi.org/10.3390/ijms21114105

Ramos, H., Soares, M. I. L., Silva, J., Raimundo, L., Calheiros, J., Gomes, C., Reis, F., Monteiro, F. A., Nunes, C., Reis, S., Bosco, B., Piazza, S., Domingues, L., Chlapek, P., Vlcek, P., Fabian, P., Rajado, A. T., Carvalho, A. T. P., Veselska, R., … Saraiva, L. (2021). A selective p53 activator and anticancer agent to improve colorectal cancer therapy. *Cell Reports*, *35*(2), 108982. https://doi.org/10.1016/j.celrep.2021.108982

Sagaert, X., Vanstapel, A., & Verbeek, S. (2018). Tumor Heterogeneity in Colorectal Cancer: What Do We Know So Far? *Pathobiology*, *85*(1–2), 72–84. https://doi.org/10.1159/000486721

Salvador, J. M., Brown-Clay, J. D., & Fornace, A. J. (2013). Gadd45 in Stress Signaling, Cell Cycle Control, and Apoptosis. In D. A. Liebermann & B. Hoffman (Eds.), *Gadd45 Stress Sensor Genes* (Vol. 793, pp. 1–19). Springer New York. https://doi.org/10.1007/978-1-4614-8289-5_1

Singh, N., Miner, A., Hennis, L., & Mittal, S. (2020). Mechanisms of temozolomide resistance in glioblastoma—A comprehensive review. *Cancer Drug Resistance*. https://doi.org/10.20517/cdr.2020.79

Souza, A. G., & C Ferreira, I. C. (2016). Advances in Cell Culture: More than a Century after Cultivating Cells. *Journal of Biotechnology & Biomaterials*, *6*(2). https://doi.org/10.4172/2155-952X.1000221

Stoyanov, G. S., Dzhenkov, D., Ghenev, P., Iliev, B., Enchev, Y., & Tonchev, A. B. (2018). Cell biology of glioblastoma multiforme: From basic science to diagnosis and treatment. *Medical Oncology*, *35*(3), 27. https://doi.org/10.1007/s12032-018-1083-x

Tawfik, E., Ahamed, M., Almalik, A., Alfaqeeh, M., & Alshamsan, A. (2017). Prolonged exposure of colon cancer cells to 5-fluorouracil nanoparticles improves its anticancer activity. *Saudi*

Pharmaceutical Journal, *25*(2), 206–213. https://doi.org/10.1016/j.jsps.2016.05.010

Wang, H.-H., Chang, T.-Y., Lin, W.-C., Wei, K.-C., & Shin, J.-W. (2017). GADD45A plays a protective role against temozolomide treatment in glioblastoma cells. *Scientific Reports*, *7*(1), 8814. https://doi.org/10.1038/s41598-017-06851-3

Wang, L., Xue, M., & Chung, D. C. (2016). C-Myc is regulated by HIF-2α in chronic hypoxia and influences sensitivity to 5-FU in colon cancer. *Oncotarget*, *7*(48), 78910–78917. https://doi.org/10.18632/oncotarget.12911

What Is Cancer? - National Cancer Institute. (n.d.). Retrieved 15 June 2021, from https://www.cancer.gov/about-cancer/understanding/what-is-cancer

Wirsching, H.-G., Galanis, E., & Weller, M. (2016). Glioblastoma. In *Handbook of Clinical Neurology* (Vol. 134, pp. 381–397). Elsevier. https://doi.org/10.1016/B978-0-12-802997-8.00023-2

Ye, X., Liu, X., Gao, M., Gong, L., Tian, F., Shen, Y., Hu, H., Sun, G., Zou, Y., & Gong, Y. (2021). CUL4B Promotes Temozolomide Resistance in Gliomas by Epigenetically Repressing CDNK1A Transcription. *Frontiers in Oncology*, *11*, 638802. https://doi.org/10.3389/fonc.2021.638802

Zhang, B., Pan, X., Cobb, G. P., & Anderson, T. A. (2007). MicroRNAs as oncogenes and tumor suppressors. *Developmental Biology*, *302*(1), 1–12. https://doi.org/10.1016/j.ydbio.2006.08.028

Zhang, J., Stevens, M. F. G., & Bradshaw, T. D. (2012). *Temozolomide: Mechanisms of Action, Repair and Resistance*. 13.

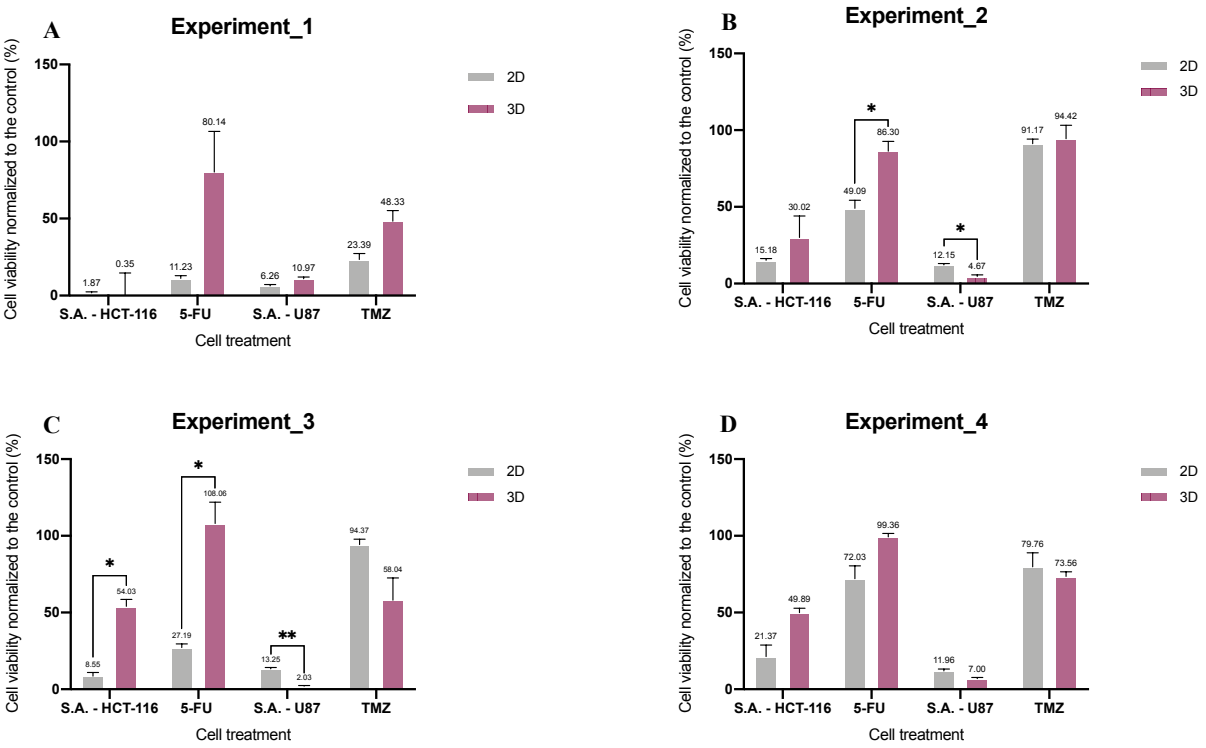

Figure 7.1 - Comparison of the percentages normalized to the control group of the cell viability of both cell lines treated in 2D and 3D cell culture models. It was performed four independent experiments as biological replicates, but since the results were not consistent between experiments it was decided to present them individually instead of in the mean form. S.A – treatment with sodium azide, as positive control of the assay; S.A. – HCT-116 – treatment with sodium azide in the HCT-116 cell line; S.A. – U87 – treatment with sodium azide in the U87-MG cell line; 5-FU – treatment with 5-FU in the HCT-117 cell line; TMZ – treatment with TMZ in the U87-MG cell line. The error bars were calculated from the SEM of the technical triplicates and the propagated error. P-values were assessed by a statistical t test and indicated as followed: P<0,033 (*), P<0,002 (**) and P<0,001 (***).

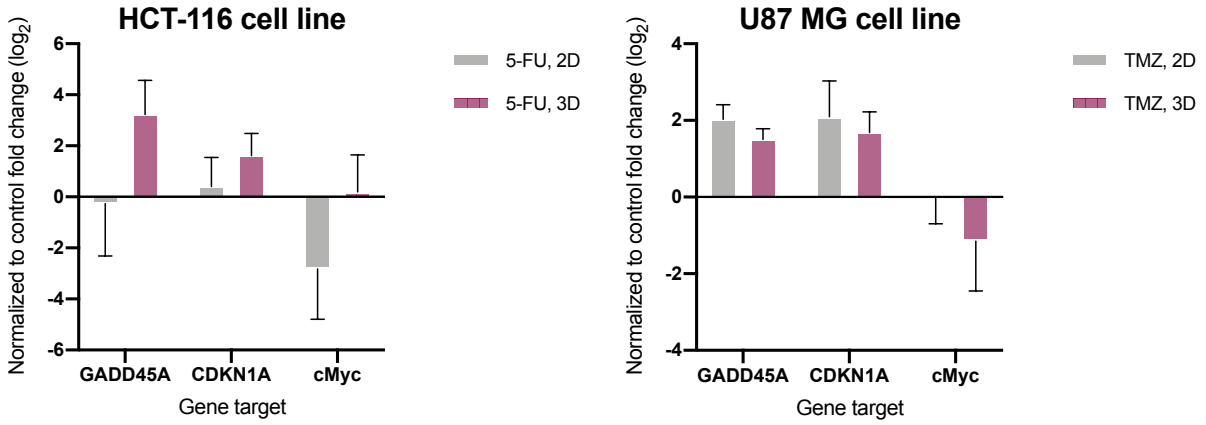

Figure 7.2 - Comparison of the GADD45A, CDKN1A and c-Myc genes fold change mean of both cell lines treated samples in 2D and 3D culture methods. It was performed the mean of the four independent biological replicates. 5-FU – treatment with 5-FU in the HCT-117 cell line; TMZ – treatment with TMZ in the U87-MG cell line. The error bars were calculated using the SEM of the biological triplicates. P-values were assessed by a statistical paired t test and indicated as followed: P<0,033 (*), P<0,002 (**), P<0,0002 (***) and P<0,0001 (****).